

# Journal of Visualized Experiments

## Radiotracer Administration for High Temporal Resolution Positron Emission Tomography (PET) of the Human Brain: Application to FDG-PET

--Manuscript Draft--

<b>Article Type:</b>	Invited Methods Article - JoVE Produced Video
<b>Manuscript Number:</b>	JoVE60259R1
<b>Full Title:</b>	Radiotracer Administration for High Temporal Resolution Positron Emission Tomography (PET) of the Human Brain: Application to FDG-PET
<b>Keywords:</b>	Positron emission tomography (PET); Fluorodeoxyglucose (FDG); constant infusion; bolus plus infusion; slow infusion; simultaneous blood oxygenation level dependent functional magnetic resonance imaging fluorodeoxyglucose positron emission tomography (BOLD-fMRI/FDG-PET); functional PET (fPET); dynamic PET
<b>Corresponding Author:</b>	Sharna Jamadar  UNITED STATES
<b>Corresponding Author's Institution:</b>	
<b>Corresponding Author E-Mail:</b>	sharna.jamadar@monash.edu
<b>Order of Authors:</b>	Sharna Jamadar Phillip GD Ward Alexandra Carey Richard McIntyre Linden Parkes Disha Sasan John Fallon Shenpeng Li Zhaolin Chen Gary F Egan
<b>Additional Information:</b>	
<b>Question</b>	<b>Response</b>
Please indicate whether this article will be Standard Access or Open Access.	Standard Access (US\$2,400)
Please indicate the <b>city, state/province, and country</b> where this article will be <b>filmed</b> . Please do not use abbreviations.	Melbourne, Victoria, Australia

**TITLE:**

**Radiotracer Administration for High Temporal Resolution Positron Emission Tomography of the Human Brain: Application to FDG-fPET**

**AUTHORS AND AFFILIATIONS:**

Sharna D. Jamadar<sup>1,2,3</sup>, Phillip G.D. Ward<sup>1,2,3</sup>, Alexandra Carey<sup>1,4</sup>, Richard McIntyre<sup>1,4</sup>, Linden Parkes<sup>1,3</sup>, Disha Sasan<sup>1</sup>, John Fallon<sup>1</sup>, Shenpeng Li<sup>1,5</sup>, Zhaolin Chen<sup>1,5</sup>, Gary F. Egan<sup>1,2,3</sup>

<sup>1</sup>Monash Biomedical Imaging, Monash University, Melbourne, Victoria, Australia

<sup>2</sup>Australian Research Council Centre of Excellence for Integrative Brain Function, Melbourne, Victoria, Australia

<sup>3</sup>Turner Institute for Brain and Mental Health, Monash University, Melbourne, Victoria, Australia.

<sup>4</sup>Department of Medical Imaging, Monash Health, Melbourne, Victoria, Australia

<sup>5</sup>Department of Electrical and Computer Systems Engineering, Monash University, Melbourne, Victoria, Australia

**Corresponding Author**

Sharna D. Jamadar (sharna.jamadar@monash.edu)

**Email Addresses of Co-Authors:**

Phillip G.D. Ward (phillip.ward@monash.edu)

Alexandra Carey (alex.carey@monash.edu)

Richard McIntyre (richard.mcintyre@monash.edu)

Linden Parkes (lindenmp@seas.upenn.edu)

Disha Sasan (disha.sasan@monash.edu)

John Fallon (john.fallon@monash.edu)

Shenpeng Li (shen.li@monash.edu)

Zhaolin Chen (zhaolin.chen@monash.edu)

Gary F. Egan (gary.egan@monash.edu)

**KEYWORDS**

positron emission tomography, PET, fluorodeoxyglucose, FDG, constant infusion, bolus plus infusion, slow infusion, simultaneous blood oxygenation level-dependent functional magnetic resonance imaging fluorodeoxyglucose positron emission tomography, BOLD-fMRI/FDG-PET, functional PET, fPET, dynamic PET

**SUMMARY:**

This manuscript describes two radiotracer administration protocols for FDG-PET (constant infusion and bolus plus infusion) and compares them to bolus administration. Temporal resolutions of 16 s are achievable using these protocols.

**ABSTRACT:**

Functional positron emission tomography (fPET) provides a method to track molecular dynamics in the human brain. With a radioactively-labelled glucose analogue, <sup>18</sup>F-fluorodeoxyglucose (FDG-

fPET), it is now possible to index the dynamics of glucose metabolism with temporal resolutions approaching those of functional magnetic resonance imaging (fMRI). This direct measure of glucose uptake has enormous potential for understanding normal and abnormal brain function and probing the effects of metabolic and neurodegenerative diseases. Further, new advances in hybrid MR-PET hardware make it possible to capture fluctuations in glucose and blood oxygenation simultaneously using fMRI and FDG-fPET.

The temporal resolution and signal-to-noise of the FDG-fPET images is critically dependent upon the administration of the radiotracer. This work presents two alternative continuous infusion protocols and compares them to a traditional bolus approach. It presents a method for acquiring blood samples, time-locking PET, MRI, experimental stimulus, and administering the non-traditional tracer delivery. Applying a visual stimulus, the protocol results show cortical maps of the glucose-response to external stimuli on an individual level with a temporal resolution of 16 s.

## **INTRODUCTION:**

Positron emission tomography (PET) is a powerful molecular imaging technique that is widely used in both clinical and research settings (see Heurling et al.<sup>1</sup> for a recent comprehensive review). The molecular targets that can be imaged using PET are only limited by the availability of radiotracers, and numerous tracers have been developed to image neural metabolism receptors, proteins, and enzymes<sup>2,3</sup>. In neuroscience, one of the most used radiotracers is <sup>18</sup>F-fluorodeoxyglucose (FDG-PET), which measures glucose uptake, usually interpreted as an index of cerebral glucose metabolism. The human brain requires a constant and reliable supply of glucose to satisfy its energy requirements<sup>4,5</sup>, and 70-80% of cerebral glucose metabolism is used by neurons during synaptic transmission<sup>6</sup>. Changes to cerebral glucose metabolism are thought to initiate and contribute to numerous conditions, including dementia, and psychiatric, neurodegenerative, and ischemic conditions<sup>7-9</sup>. Furthermore, as FDG uptake is proportional to synaptic activity<sup>10-12</sup>, it is considered a more direct and less confounded index of neuronal activity compared to the more widely used blood oxygenation level-dependent functional magnetic resonance imaging (BOLD-fMRI) response. BOLD-fMRI is an indirect index of neural activity and measures changes in deoxygenated hemoglobin that occur following a cascade of neurovascular changes following neuronal activity.

Most FDG-PET studies in the human brain acquire static images of cerebral glucose uptake. The participant rests quietly for 10 min with their eyes open in a darkened room. The full radiotracer dose is administered as a bolus over a period of seconds, and the participant then rests for a further 30 min. Following the uptake period, participants are placed in the center of the PET scanner, and a PET image that reflects the cumulative FDG distribution over the course of the uptake and scanning periods is acquired. Thus, the neuronal activity indexed by the PET image represents the cumulative average of all cognitive activity over uptake and scan periods and is not specific to cognitive activity during the scan. This method has provided great insight into the cerebral metabolism of the brain and neuronal function. However, the temporal resolution is ~45 min, effectively yielding a static measurement in comparison to cognitive processes and current common experiments in neuroimaging. Due to the limited temporal resolution, the method

provides a non-specific index of glucose uptake (i.e., not locked to a task or cognitive process) and cannot provide measures of within-subject variability, which can lead to erroneous scientific conclusions due to Simpson's Paradox<sup>13</sup>, where brain-behavior relationships calculated across-subjects are not necessarily indicative of the same relationships tested within-subjects. Furthermore, recent attempts to apply functional connectivity measures to FDG-PET can only measure across-subjects connectivity. Thus, differences in connectivity can only be compared between groups and cannot be calculated for individual subjects. While it is debatable what exactly across-subject connectivity measures<sup>14</sup>, it is clear that measures calculated across—but not within—subjects cannot be used as a biomarker for disease states or used to examine the source of individual variation.

In the past five years, the development and wider accessibility of clinical-grade simultaneous MRI-PET scanners has sparked renewed research interest in FDG-PET imaging<sup>2</sup>. With these developments, researchers have focused on improving the temporal resolution of FDG-PET to approach the standards of BOLD-fMRI (~0.5–2.5 s). Note that the spatial resolution of BOLD-fMRI can approach submillimeter resolutions but the spatial resolution of FDG-PET is fundamentally limited to around 0.54 mm full width at half maximum (FWHM) due to the positron range<sup>15</sup>. Dynamic FDG-PET acquisitions, which are often used clinically, use the bolus administration method and reconstruct the list-mode data into bins. The bolus dynamic FDG-PET method offers a temporal resolution of around 100 s (e.g., Tomasi et al.<sup>16</sup>). This is clearly much better compared to static FDG-PET imaging but is not comparable to BOLD-fMRI. Additionally, the window in which brain function may be examined is limited, because the blood plasma concentration of FDG diminishes.

To expand this experimental window, a handful of studies<sup>17–21</sup> have adapted the radiotracer infusion method previously proposed by Carson<sup>22,23</sup>. In this method, sometimes described as 'functional FDG-PET' (FDG-fPET, analogous to BOLD-fMRI), the radiotracer is administered as a constant infusion over the course of the entire PET scan (~90 min). The goal of the infusion protocol is to maintain a constant plasma supply of FDG to track dynamic changes in glucose uptake across time. In a proof-of-concept study, Villien et al.<sup>21</sup> used a constant infusion protocol and simultaneous MRI/FDG-fPET to show dynamic changes in glucose uptake in response to checkerboard stimulation with a temporal resolution of 60 s. Subsequent studies have used this method to show task-locked FDG-fPET (i.e., time-locked to an external stimulus<sup>19</sup>) and task-related FDG-fPET (i.e., not time-locked to an external stimulus<sup>17,18</sup>) glucose uptake. Using these methods, FDG-fPET temporal resolutions of 60 s have been obtained, which is a substantial improvement over bolus methods. Preliminary data show that the infusion method can provide temporal resolutions of 20–60 s<sup>19</sup>.

Despite the promising results from the constant infusion method, the plasma radioactivity curves of these studies show that the infusion method is not sufficient to reach a steady-state within the timeframe of a 90 min scan<sup>19,21</sup>. In addition to the constant infusion procedure, Carson<sup>22</sup> also proposed a bolus/infusion procedure, where the goal is to quickly reach equilibrium at the beginning of the scan, and then sustain plasma radioactivity levels at equilibrium for the duration of the scan. Rischka et al.<sup>20</sup> recently applied this technique using a 20% bolus plus 80% infusion.



As expected, the arterial input function quickly rose above baseline levels and was sustained at a higher rate for a longer time, compared to results using an infusion-only procedure<sup>19,21</sup>.

This paper describes the acquisition protocols for acquiring high temporal resolution FDG-*f*PET scans using infusion-only and bolus/infusion radiotracer administration. These protocols have been developed for use in a simultaneous MRI-PET environment with a 90–95 min acquisition time<sup>19</sup>. In the protocol, blood samples are taken to quantify plasma serum radioactivity for subsequent quantification of PET images. While the protocol's focus is the application of infusion methods for functional neuroimaging using BOLD-*f*MRI/FDG-*f*PET, these methods can be applied to any FDG-*f*PET study regardless of whether simultaneous MRI, BOLD-*f*MRI, computed tomography (CT), or other neuroimages are acquired. **Figure 1** shows the flowchart of procedures in this protocol.

## **PROTOCOL:**

This protocol has been reviewed and approved by the Monash University Human Research Ethics Committee (approval number CF16/1108 – 2016000590) in accordance with the Australian National Statement on Ethical Conduct in Human Research<sup>24</sup>. Procedures were developed under the guidance of an accredited Medical Physicist, Nuclear Medicine Technologist, and clinical radiographer. Researchers should refer to their local experts and guidelines for the administration of ionizing radiation in humans.

### **1. Required equipment and personnel**

1.1. See the **Table of Materials** for the scanner room, radiochemistry lab, and general materials. A commercial supplier was used for the radiotracer.

1.2. In the simultaneous MRI-PET environment, use four personnel: a radiographer (RG) to run the scan, a nuclear medicine technologist (NMT) to oversee the administration of the radiotracer and acquisition of blood samples, a laboratory assistant (LA) to spin blood, and a research assistant (RA) responsible to oversee the experimental design and stimulus presentation.

## **2. Preparation**

### **2.1. Tracer dose preparation by the NMT**

2.1.1. Calculate the infusion volume that will be administered over the course of the scan. In this protocol, the rate of infusion is 0.01 mL/s over 95 min. So, in a 95 min scan, participants receive  $0.01 \text{ mL/s} \times 60 \text{ s} \times 95 \text{ min} = 57 \text{ mL}$ .

2.1.2. Calculate the tracer dose that will be diluted into the administered saline solution. In this protocol, a total dose of 260 MBq is administered to the participant over 95 min. This dose was chosen to limit radiation exposure to 4.9 mSv, to keep within the 'low level risk' categorization according to Australian Radiation Protection and Nuclear Safety Agency (ARPANSA) guidelines

for exposure of humans to ionizing radiation<sup>25</sup>. Decay correct 260 MBq from the mid-infusion point (47.5 min) back to  $T_0$ . Using Equation 1, solve for  $A_0$ :

$$A_t = A_0 \cdot e^{\lambda t}$$

Where  $A_t$  is the radioactivity (MBq) at the mid-timepoint of the infusion,  $A_0$  is the initial radioactivity, and  $\lambda$  is the radioactive decay constant specific to the tracer. For FDG, the value of  $\lambda$  is  $\approx 0.693/T_{1/2}$ .  $T_{1/2}$  is the half-life of  $^{18}\text{F}$  (110 min).

NOTE: In this example,  $A_t = 260$  MBq,  $\lambda = 0.693/110$ , and  $t = -47.5$ , so  $A_0 = 350.942$  MBq.

**2.1.3. Calculate the required radiotracer dose for the 100 mL saline bag that will be used to administer the dose to the participant. The required radiotracer for the saline bag is diluted up to a total volume of 5 mL and drawn up in a 5 mL syringe. Therefore, for the 100 mL saline bag, the dilution factor is the volume of saline (100 mL) in addition to the 5 mL volume of the syringe with radiotracer. This total volume of 105 mL is divided by the infusion volume of 57 mL (i.e., 105 mL/57 mL = 1.842). So, the total radioactivity in a volume of 5 mL required for addition to the 100 mL bag is  $A_0 \times$  the dilution factor (i.e., 350.942 MBq  $\times$  1.842 = 646.44 MBq). Aseptically add the radiotracer to the saline bag.**

NOTE: It is important to note that the calculated activity of 646.44 MBq that is added to the saline bag is the activity required at the commencement of the infusion. Generally, the doses for this protocol are prepared between 15 min to 1 h before administration. Therefore, it is important to factor in the decay of the radioisotope. Equation 1 in 2.1.2. can be used to account for this, where time (t) is the total number of minutes from the preparation of the dose to when the activity will be administered,  $A_t = 646.44$  MBq, by solving for  $A_0$ .

**2.1.4. Prepare the priming dose. Withdraw 20 mL from the bag into a syringe and cap it. Calibrate this 20 mL syringe and label.** The syringe is calibrated as a reference check to ensure that the radioactivity has evenly dispersed within the saline bag.

**2.1.5. Prepare the dose. Using a 50 mL syringe, withdraw 60 mL from the bag and cap with a red Combi stopper.** This syringe is not calibrated, as the concentration of the radioactivity is known from the time it was added to the saline bag (step 2.1.3). **Store both syringes in the radiochemistry lab until ready to scan.**

NOTE: It is possible to draw a 60 mL volume in a 50 mL syringe, because Terumo syringes are marked to 20% above the labelled volume (i.e., a 50 mL syringe is marked to 60 mL).

**2.1.6. Prepare the reference dose. Fill a 500 mL volumetric flask with approximately 480 mL of distilled water. Draw up 10 MBq of  $^{18}\text{F}$ -FDG into a syringe, decay-corrected to the scan start time (using Equation 1) and add it to the flask. Top the volume up to the 500 mL mark with more distilled water and mix thoroughly. Affix labels pre- and post-calibration for the syringe.**

## 2.2. Scanner room preparation by the NMT

2.2.1. Once the participant is positioned in the scanner, there is very little room to manipulate or salvage the line for infusion or blood samples if blockage occurs. Prepare the scanner room to minimize the chance of line blockage.

2.2.2. Ensure that all blood-collection equipment is within easy reach of the collection site. Place underpads at the end of the cannula and on any surface that will hold blood containers. Place bins for regular waste and biohazardous waste within easy reach of the blood collection site.

## 2.3. Infusion pump preparation by the NMT

2.3.1. Set up the infusion pump in the scanner room on the side that will be connected to the participant. Build lead bricks around the base of the pump and place the lead shield in front of the pump. Connect the tubing for the infusion pump that delivers the infusion to the participant and ensure the correct infusion rate has been entered. For this protocol, the rate is 0.01 mL/s.

2.3.2. Prime the tubing before it is connected to the participant's cannula. Connect the 20 mL priming dose to the infusion pump. On the end of the tubing that will be connected to the participant, attach a three-way tap and an empty 20 mL syringe. Ensure that the tap is positioned to allow the  $^{18}\text{F}$ -FDG solution to flow from the priming dose through the tubing and collect only into the empty syringe.

2.3.3. Preset the infusion pump to prime a volume of 15 mL. Select the **Prime** button on the pump and follow the prompts to prime the line.

2.3.4. Attach the 50 mL dose syringe to the infusion pump in place of the priming dose. The 15 mL primed dose on the three-way tap can remain there until the participant is ready to be connected to the pump.

## 2.4. Participant preparation by the NMT, RA, and RG

2.4.1. Advise participants to fast for 6 h, and to consume only water (approximately two glasses), prior to the scan.

2.4.2. Have the RA conduct the consent procedures and acquire additional measures (e.g., demographic surveys, cognitive batteries, etc.). Have the NMT and RG conduct the safety screens, the NMT review safety for PET scanning (e.g., exclusion for pregnancy, diabetes, chemotherapy or radiotherapy in the previous 8 weeks, and known allergies), and the RG review participant safety for MRI scanning (e.g., exclusion for pregnancy, medical or non-medical metallic implants, non-removable dental implants, claustrophobia).

2.4.3. Cannulate the participant.

2.4.3.1. Use two cannulas: one for dose administration and the other for blood sampling. The most appropriate cannula varies across participants, but the most suitable vein should be reserved for blood collection. A 22 G cannula is the preferred minimum size. Collect a 10 mL baseline blood sample while cannulating. Disconnect all saline flushes under pressure to maintain patency of the line.

2.4.3.2. Test the participant's blood sugar level and other baseline blood measures (e.g., hemoglobin) from the baseline sample.

## 2.5. Participant positioning in the scanner by the RG and NMT

2.5.1. Have the RG position the participant in the scanner bore. For long scans, it is imperative to ensure comfort in order to reduce the risk of the participant dropping out and motion artefact due to discomfort. The participant should be covered with a disposable blanket to maintain a comfortable body temperature.

2.5.2. Have the NMT flush the cannula to ensure it is patent with minimal resistance before connecting the infusion line. Once connected, the tubing can be lightly taped near the wrist. Instruct the participant to keep their arm straightened. Use supports such as foam or cushions for comfort. Have the NMT also check the cannula that will be used for plasma samples to ensure that it is able to withdraw blood with minimal resistance. It may be necessary to connect an extension tube primed with normal saline to make the cannula more accessible while the participant is in the scanner. If this is required, it should be checked for leakages.

2.5.3. Once the subject is in the scanner bore, have the NMT check that they have suitable access to both cannulas.

2.5.4. Have the NMT notify the RG and RA if there are any issues with the blood collection cannula, infusion cannula, or the infusion pump (e.g., occlusion, battery, extravasation) at any time during the scan.

## 3. Scan the participant

### 3.1. Starting the scan with the NMT, RG, and RA

3.1.1. At the start of the scan, situate the NMT in the scanner room to monitor the infusion equipment. Ensure the NMT is wearing hearing protection and using the barrier shield to minimize radiation exposure from the dose where possible.

3.1.2. As the RG performs the localizer scan to ensure that the participant is in the correct position, check the details for the PET acquisition (e.g., scan duration, list-mode data collection, correct isotope).

3.1.3. Design the protocol so that the PET acquisition will commence with the first MRI sequence. The RG prepares and starts the MRI sequence. The start time of the 95 min PET acquisition is time-locked to the start of the MRI sequence. If required, the NMT should deliver the bolus at the time of PET acquisition (**Figure 1**).

3.1.4. Start the infusion pump. The RG should signal the NMT (e.g., via a thumbs-up sign) to start the pump 30 s after the start of the PET acquisition. This protocol starts the infusion pump 30 s after the scan start time to provide a safety buffer in case of scan failure. This also ensures that the first image taken during the PET scan indexes the brain prior to radiotracer administration for complete time activity curve data collection. Have the NMT observe the pump to ensure it has started to infuse the  $^{18}\text{F}$ -FDG and that there is no immediate occlusion of the line.

3.1.5. Have the RA initiate any external stimulus at the agreed upon time (i.e., at the start of a functional run/experimental block) and calculate the times for blood samples. An example record form is shown in **Supplement 1**. Have the RA calculate the predicted time of each blood sample and provide copies to the NMT and lab assistant (LA). Have the RA ensure that the NMT takes the blood samples at approximately the correct time, and monitors equipment (e.g., infusion pump, stimulus) for any signs of errors.

## 3.2. Take blood samples at regular time intervals.

3.2.1. Have the NMT and RA take one sample every 10 min. There are usually 10 samples in total, not including the baseline sample.

3.2.2. If acquiring MRI scans simultaneously with PET scans, have the NMT wear hearing protection when entering the scanner room.

3.2.3. Have the NMT wear gloves and swab the tip of the cannula clean. While the cannula site dries, open a 5 mL and a 10 mL syringe, vacutainer, and a 10 mL saline flush.

3.2.4. Using the 5 mL syringe, withdraw 4–5 mL of fresh blood and discard the syringe in the biohazard waste.

3.2.5. Using the 10 mL syringe, withdraw up to 10 mL of blood. The volume may be limited by how easily the blood can be withdrawn. It is important to minimize any resistance subsequently causing damage to the red blood cells that can hemolyze. At the midcollection point, have the NMT signal to the RA, who will mark this time on the record form (**Supplement 1**) as the 'actual' time of sample.

3.2.6. Connect the 10 mL syringe to the vacutainer and then deposit the blood into the relevant blood tube.

3.2.7. Quickly flush the cannula with 10 mL of saline, disconnected under pressure, to minimize any chance of line clotting.

3.2.8. Immediately take the blood sample to the radiochemistry lab for analysis.

### 3.3. Spinning the blood by the LA

3.3.1. Have the LA get all the equipment ready (**Table 1**) and be wear gloves. Have three racks set out for the samples: one for blood tubes, one for pipetting the sample, and one for filled pipetted samples (pre- and post-counting).

3.3.1.1. Have the LA regularly change gloves throughout the procedure, especially when handling the counting tube. If the LA has any radioactive plasma contamination on their gloves, it can be transferred to the counting tube and spuriously increase the number of recorded counts of the sample.

3.3.2. The blood sample can be placed in the centrifuge as the availability of staffing resources permits, because the time that the blood sample was taken, and the time it was counted was noted. Spin all samples at a relative centrifugal force of  $724 \times g$ . The centrifuge settings used for this protocol are 2,000 rpm for 5 min with the acceleration and deceleration curves set to eight.

3.3.3. Once the sample has been spun, place the tube in the pipetting rack. Remove the tube cap to not disturb sample separation. Place a labelled counting tube in the rack. The label should correspond to the blood tube.

3.3.4. Ensure the tip is securely fastened to the pipette. Have a tissue ready for any drips. Steadily pipette 1,000  $\mu\text{L}$  of plasma from the blood tube, transfer to the counting tube, and replace the lids on the counting tube and blood tube.

3.3.5. Place the counting tube into the well counter and count for 4 min. Record the counting start time on the record sheet ('measurement time') for every sample. This is required for subsequent corrections to the PET acquisition start time. At later time points during the scan, have the LA perform each step in rapid succession to avoid a backlog of samples.

3.3.6. Dispose of any blood product waste in biohazard bags.

## REPRESENTATIVE RESULTS:

### Study-specific methods

Here, study-specific details for the representative results are reported. These details are not critical to the procedure and will vary across studies.

### Participants and task design

Participants ( $n = 3$ , **Table 2**) underwent a simultaneous BOLD-fMRI/FDG-fPET study. As this manuscript focuses on the PET acquisition protocol, MRI results are not reported. Participants received 260 MBq of  $^{18}\text{F}$ -FDG over the course of a 95 min scan. Participant 1 received the full dose as a bolus at the start of the scan. Participant 2 received the dose in an infusion-only

protocol. Participant 3 received the same dose with a hybrid 50% bolus plus 50% infusion. For both infusion-only and bolus/infusion protocols, infusion duration was 50 min.

The task was presented in an embedded block design (**Figure 2**)<sup>19</sup>. This design was previously shown to provide simultaneous contrast for task-evoked BOLD-fMRI and FDG-fPET data. Briefly, the task alternated between 640 s flashing checkerboard blocks and 320 s rest blocks. This slow alternation provides FDG-fPET contrast. These timing parameters were entered into the first-level general linear models during the analysis. Within the 640 s checkerboard blocks, checkerboard and rest periods alternated at a rate of 20 s on/20 s off. This fast alternation, which is suited to BOLD-fMRI, will hopefully be detectable with FDG-fPET with future analysis and reconstruction advances. In this protocol, rest periods were with eyes open, fixated on a cross centrally presented on the screen.

### Image acquisition and processing

MR and PET images were acquired on a Siemens 3T Biograph mMR. PET data were acquired in list mode. The MRI and PET scans were acquired in the following order (details provided only for images relevant to the current manuscript): (i) T1-weighted 3D MPRAGE (TA = 7.01 min, TR = 1,640 ms, TE = 2.34 ms, flip angle = 8°, FOV = 256 x 256 mm<sup>2</sup>, voxel size = 1 x 1 x 1 mm<sup>3</sup>, 176 slices, sagittal acquisition; (ii) T2-weighted FLAIR (TA = 5.52 min); (iii) QSM (TA = 6.86 min); (iv) gradient field map TA = 1.03 min; (v) MR attenuation correction Dixon (TA = 0.39 min, TR = 4.1 ms, TE<sub>in phase</sub> = 2.5 ms, TE<sub>out phase</sub> = 1.3 ms, flip angle = 10°); (vi) T2\*-weighted echo-planar images (EPIs) (TA = 90.09 min), P-A phase correction (TA = 0.36 min); (vii) UTE (TA = 1.96 min). The onset of the PET acquisition was locked to the onset of the T2\* EPIs.

T1-weighted structural images were neck-cropped using FSL-robustfov<sup>26</sup>, bias corrected using N4<sup>27</sup>, and brain extracted using ANTs<sup>28,29</sup> with OASIS-20 templates<sup>30,31</sup>. T1-weighted images were non-linearly normalized to a 2 mm MNI template using ANTs<sup>32</sup> with the default parameter set defined by antsRegistrationSyN.sh.

This manuscript examined dynamic FDG-fPET results with bin size 16 s. All data were reconstructed offline using Siemens Syngo E11p and corrected for attenuation using pseudoCT<sup>33</sup>. The ordinary Poisson ordered subset expectation maximization (OP-OSEM) algorithm with point spread function (PSF) modelling<sup>34</sup> was used with three iterations, 21 subsets, and 344 x 344 x 127 (voxel size: 2.09 x 2.09 x 2.03 mm<sup>3</sup>) reconstruction matrix size. A 5-mm 3D Gaussian post-filtering was applied to the final reconstructed images.

Spatial realignment was performed on the dynamic FDG-fPET images using FSL MCFLIRT<sup>35</sup>. A mean FDG-PET image was derived from the entire dynamic timeseries and rigidly normalized to the individual's high-resolution T1-weighted image using advanced normalization tools (ANT)<sup>32</sup>. The dynamic FDG-fPET images were then normalized to MNI space using the rigid transform in combination with the non-linear T1 to MNI warp.

First-level general linear models were estimated using SPM12 (Wellcome Centre for Human Neuroimaging) with the event time-course (checkerboard on, fixation) modelled as the effect of

interest. Average uptake across a control region, the frontopolar cortex (left and right FP1/2<sup>36</sup>), was included as a covariate. The model did not include global normalization, high-pass filter, convolution with the hemodynamic response, autoregressive model, or masking threshold. An explicit mask of the visual cortex in hOC1–5 (left and right hOC1,2,3d,3v,4d,4la4lp,4v,5<sup>37–39</sup>; SPM Anatomy Toolbox v 2.2b<sup>40–42</sup>) was included in the model to restrict the model estimation to regions of interest (ROI). In the clinical environment, multiple regions are analyzed using brain atlases. T contrasts were used to estimate parameter maps of the individual-level activity, liberally thresholded at  $p = 0.1$  (uncorrected),  $k = 50$  voxels. The results for each individual are also shown at multiple thresholds in **Supplement 2**.

### **Plasma radioactivity concentration results**

The plasma radioactivity concentration curve for each participant is given in **Figure 3**. The largest peak plasma radioactivity concentration (3.67 kBq/mL) was obtained using the bolus method. Visual inspection of **Figure 3** shows that the peak occurs within the first 10 min of the protocol, and the concentration decreases thereafter. Note that protocols that use arterial or automated sampling at a rate of less than 1 min will likely find a peak plasma concentration within the first minute. The delay here is because the first blood sample was taken at 5 min post-bolus. By the end of the recording period, the plasma radioactivity was 35% of the peak (1.28 kBq/mL). The infusion-only protocol reached maximum (2.22 kBq/mL) at 50 min, the end of the infusion period. By the end of the recording period, the concentration was sustained at 68% of its peak (1.52 kBq/mL). Like the bolus-only protocol, the bolus/infusion protocol reached its peak plasma radioactivity concentration (2.77 kBq/mL) within the first 5 min. By the end of the recording period, bolus/infusion concentration was at 53% of the peak (1.49 kBq/mL).

Qualitatively, plasma radioactivity levels were sustained for the longest duration in the bolus/infusion protocol. Both infusion-only and bolus/infusion protocols show an apparent reduction in radioactivity when the infusion period ends (50 min). Visually comparing bolus-only and bolus/infusion protocols, plasma radioactivity was smaller in bolus-only vs. bolus/infusion by 40 min post-injection. Critically, the plasma radioactivity was minimally varied for a period of approximately 40 min in the bolus/infusion protocol. In contrast, neither the infusion-only nor bolus-only protocol exhibit a qualitatively sustained period of consistent activity.

### **PET Signal Results**

Individual-level parameter maps from the general linear model, PET signal and GLM fitted response, and errors are shown in **Figure 4**. Parameter maps are also shown at different statistical thresholds in **Supplement 2**.

**Figure 4ii** shows the PET signal across the scan period (i.e., across stimulation and rest periods) in the bilateral visual cortex (hOC1–5) and in the control region (frontal pole, FP1/2) for the three administration protocols. Qualitatively, the bolus/infusion participant showed clearer differences between the ROIs, compared to bolus-only and infusion-only participants. For the bolus/infusion protocol, the frontopolar ROI showed the highest image intensity, with the lowest for hOC4. For the bolus-only participant, there was a similar trend, with hOC5 and FP1/2 showing the highest



intensity, with hOC4 showing the lowest. For the infusion-only participant, the FP1/2 and right hOC5 showed the highest intensity, with little difference between the remaining ROIs.

Visual inspection of **Figure 4ii** suggests that in the bolus-only protocol, there is a sharp increase in signal following the bolus. The slope of the uptake is relatively fast in the next 20–30 min, but the rate of uptake decreases in the remainder of the measurement period. In the bolus/infusion protocol, there is a sharp increase in uptake at the start of the scan that is of smaller magnitude than in the bolus-only protocol, and the uptake continues at a comparatively faster rate for the duration of the scan. By the end of the recording period, the bolus/infusion protocol shows a larger uptake than the bolus-only protocol. By comparison, the infusion-only protocol shows low signal for the first 40 min of the scan, and the peak uptake is substantially lower than the bolus-only or bolus/infusion protocol. Uptake is fastest in the first ~50 min of the scan and slows for the remainder of the recording period.

#### **Parameter Maps and Fitted Response Results**

**Figure 4i** shows the individual-level T maps for the three administration protocols. **Figure 4iii** shows the general linear model fitted response and error at the peak voxel for each subject. Note that for the infusion-only protocol (**Figure 4Biii**), the scale is larger than for the bolus-only and bolus/infusion protocols. Furthermore, for the infusion-only protocol, the signal during the first rest block was close to zero, as very little of the tracer had been administered during that time, and the general linear model estimation failed when considering this block. Thus, the general linear model was estimated for this participant starting with the first task block, and the fitted response is shown from the start of the first checkerboard period.

To visualize the task effects across time, the time course data for each subject was extracted (first eigenvariate) and the inverse of the coefficient of variation (mean/standard deviation) was calculated for each block. The inverse of the coefficient of variation approximates the signal-to-noise ratio. As can be seen from **Figure 5**, the signal increased roughly linearly across the recording period for the three protocols. The slope of the line was highest for the infusion-only protocol ( $m = 2.794$ ), intermediate for the bolus-only (1.377) and smallest for the bolus/infusion protocol (1.159).

#### **FIGURE AND TABLE LEGENDS:**

**Figure 1. Flowchart of procedures for FDG-fPET experiments.** Top: procedures for prescreening of participants prior to study recruitment. Bottom: procedures for the bolus-only (left), infusion-only (center), and bolus/infusion (right) protocols. The staff member responsible for each procedure is listed in parentheses. Section identifiers refer to the sections in the text where the procedure is described. \*EXCL indicates timepoints when participants may be excluded, either for MR or PET scanning incompatibility, or not meeting study entry requirements (e.g., cognitive and psychological requirements). NMT = Nuclear Medicine Technologist, RA = Research Assistant, RG = Radiographer, LA = Lab Assistant.

**Figure 2. Timing parameters and the predicted plasma radioactivity from the three protocols.** Red, green, and blue traces represent the hypothesized plasma radioactivity curves for the bolus,

infusion, and bolus/infusion protocols, respectively. Note that these traces are for illustrative purposes only. See **Figure 3** for obtained plasma radioactivity curves. The timing parameters are superimposed to show the relative timing of the task relative to the expected plasma radioactivity. The embedded block design (Jamadar et al. 2019<sup>19</sup>) has a slow alternation (10/5 min) between checkerboard stimulation and eyes-open rest. Embedded within the ‘on’ blocks is a fast alternating (20 s) on/off design. The slow alternation provides FDG-fPET contrast. The fast alternation provides BOLD-fMRI contrast.

**Figure 3. Plasma radioactivity curves for the three participants.** Decay was corrected to the time the blood was sampled. The arrow indicates the cessation of the infusion for the infusion-only and bolus/infusion protocols. Time is in minutes.

**Figure 4. Individual-level parameter maps from the general linear model, PET signal, and GLM fitted response and error.** (i) Individual-level statistical parameter (T) maps for each of the three subjects, thresholded at  $p$  (uncorrected)  $< 0.1$ ,  $k = 50$  voxels. (ii) PET signal across the visual cortex in regions of interest: five occipital (left and right hOC1, hOC2, average hOC3d/3v, average 4d/4la/4lp/4v, hOC5) and frontal (left and right average FP1/2) control areas. Note that the left regions are shown in solid lines, right regions shown in dotted lines. (iii) Model fit and error across time for the peak of activity in each subject. Arrow shows the end of the infusion period. (Aiii) bolus-only peak activity MNI coordinate (-24, -100, 12),  $T = 4.07$ ; infusion-only (Biii) peak activity MNI coordinate (10, -86, 12),  $T = 4.25$ ; bolus/infusion peak activity coordinate (26, -65, -10),  $T = 5.17$ . Note that for the infusion-only protocol, the model could not be estimated for the first rest period due to a very low signal. Also note the larger scale for the infusion-only protocol compared to the bolus-only and bolus/infusion protocols.

**Figure 5. Signal to noise ratio across the recording period.** The plot shows the inverse of the coefficient of variation (mean/SD) of the first eigenvariate of the activity within the peak voxel in each checkerboard block. SD = standard deviation.

**Table 1. Demographic information for the three participants.**

**Supplement 1. Example participant record form.** In this protocol, the RA is responsible for recording the time of bolus and infusion start and calculating the time of blood samples. The RA then provides copies of this form to the NMT and LA. During the experiment, the RA records the times that the samples were taken for subsequent decay correction. The LA records the time of measurement and the measurement values in the Notes section.

**Supplement 2. Variability in statistical parameter maps with different statistical thresholds.** Results are presented in slices at a range of thresholds from  $p = 1.0$  to FWE  $p < 0.05$ .

## DISCUSSION:

FDG-PET is a powerful imaging technology that measures glucose uptake, an index of cerebral glucose metabolism. To date, most neuroscience studies using FDG-PET use a traditional bolus administration approach, with a static image resolution that represents the integral of all

metabolic activity over the course of the scan<sup>2</sup>. This manuscript describes two alternative radiotracer administration protocols: the infusion-only (e.g., Villien et al., Jamadar et al.<sup>19,21</sup>) and the hybrid bolus/infusion (e.g., Rischka et al.<sup>20</sup>) protocols. The three protocols demonstrated a temporal resolution of 16 s, time-locked to a stimulus, at the individual-level.

The critical point in the method is the start of the scanning protocol. At this point, the beginning of the PET acquisition must be time-locked to the beginning of the BOLD-fMRI sequence (if using simultaneous MR-PET), as well as the start of the stimulus presentation. Stimulus onsets and durations must be able to be locked to the onset of the scan for the first-level models. In the bolus-only protocol, the bolus should be delivered at the beginning of the PET acquisition to capture the peak signal (**Figure 4**). In the infusion-only protocol, the beginning of the infusion should be locked to the PET acquisition, to ensure accurate modelling of the uptake at the first-level. In the bolus/infusion protocol, the bolus should be time-locked to the PET acquisition, with the infusion starting at a known, short period, after the bolus. In order for the procedures to flow correctly within this short time period, each of the staff members (NMT, RG, RA) should be adequately prepared prior to the start of the scan (**Figure 1**). Dress rehearsals are recommended to choreograph the timing of this critical stage.

To date, approximately 60 subjects have been tested using one of these protocols (the largest number using the infusion-only protocol). There are two common causes of subject attrition or acquisition failure. (1) Researchers are unable to cannulate the participant due to difficulty finding veins. To address this, all participants must drink at least two glasses of water before the scan. If only one cannula can be achieved, blood sampling is omitted for that participant. (2) Participants are unable to complete the scan. Unlike MRI, the PET acquisition cannot be paused and restarted. The most common causes of in-scan participant withdrawal are due to toilet breaks and difficulty with thermal regulation. Participants have reported that the requirement to consume water before the scan increases the need to urinate. Thus, all participants are required to do so prior to scanning. Participants have also reported that the infusion of the tracer leaves them feeling very cold, and shivering is triggered in some people. Previous studies have shown that ambient temperature can influence artefactual activity in FDG-PET scans<sup>46</sup>. This issue is addressed by using a disposable quilt for all participants during the scan.

Results are shown at the individual subject level for the three administration protocols. As expected, the blood plasma radioactivity concentration (**Figure 3**) had the largest peak for the bolus-only protocol, but the most sustained radioactivity in the bolus/infusion protocol. The plasma concentration was lowest for the infusion-only protocol. For both the infusion-only and bolus/infusion protocols, the concentration decreased at the time the infusion ceased. PET signal across the ROIs (**Figure 4Bii**) showed the largest signal in the bolus/infusion protocol. This participant also showed the clearest differentiation between the ROIs. Qualitatively, the PET signal was weakest in the infusion-only protocol. It is possible that the infusion-only protocol would yield better results in a longer experiment (>50 min). However, this would likely increase the rate of participant attrition. In the first-level general linear models, model error was much greater in the infusion-only protocol compared to the bolus-only and bolus/infusion protocols (**Figure 4iii**). Signal-to-noise during the task periods (**Figure 5**) suggested that the most stable

signal across the recording period was obtained using the bolus/infusion protocol. Further studies are required to determine if these effects are sustained in a larger sample.

fPET is a relatively new method (first published by Villien et al.<sup>21</sup>), and the data are relatively complex to acquire compared to traditional neuroimaging approaches like static PET and MRI/fMRI. Thus, there is substantial room for improvement for the data acquisition protocols. This study presents the acquisition protocol for three tracer administration protocols (bolus-only, infusion-only, and bolus plus infusion) and the representative results from individual subjects for each method. In this group, no arterial sampling was performed due to the invasiveness of the procedure and the requirement for an MD on site. Our image analyses therefore do not benefit from the quantitative information provided by arterial sampling. Note that Hahn et al.<sup>17</sup> found excellent agreement between arterial and venous sampling for determining cortical cerebral metabolic rate of glucose (CMRGlc) for constant infusion FDG-fPET. Other published works<sup>43–45</sup> discuss arterial, venous, and image-derived input functions for PET in detail.

Manual blood sampling, whether arterial or venous, requires staff to enter the scanner room while scanning is underway. Most scanners have an RF interlock for the scanner room, which enables staff to access the room during scanning without causing electromagnetic interference artefacts in the MR images. However, staff entering the room during the scan may increase the radiation exposure to staff, cause participant discomfort, and increase participant movement and disengagement from cognitive tasks. These factors encourage the collection of as few samples as necessary. Taking samples every 5–10 min while the dose is administered is sufficient to observe the low-frequency blood dynamics expected from the three protocols examined here. However, this sampling rate limits the ability to quantify high-frequency temporal characteristics, particularly the exact size and shape of the peak following bolus administration. Where such characteristics are of importance, the use of automated blood sampling equipment may be beneficial.

Lastly, traditional PET modelling methods were developed for static imaging (e.g., kinetic, Patlak). More work is required to update the mathematical models for application to fPET data.

In summary, this manuscript presents alternative methods of FDG radiotracer administration for high temporal resolution FDG-PET, with a resolution of 16 s. This temporal resolution compares favorably to current standards in the literature. Hahn et al., Jamadar et al., and Villien et al.<sup>17–19,21</sup> report FDG-fPET with 1 min resolution, and Rischka et al.<sup>20</sup> achieved stable FDG-fPET results with a frame duration of 12 s using 20/80% bolus plus infusion. The bolus/infusion protocol presented here appears to provide the most stable signal for the longest period of time compared to the bolus-only and infusion-only protocols.

#### **ACKNOWLEDGEMENTS:**

Jamadar is supported by an Australian Council for Research (ARC) Discovery Early Career Researcher Award (DECRA DE150100406). Jamadar, Ward, and Egan are supported by the ARC Centre of Excellence for Integrative Brain Function (CE114100007). Chen and Li are supported by funding from the Reignwood Cultural Foundation.

Jamadar, Ward, Carey, and McIntyre designed the protocol. Carey, McIntyre, Sasan, and Fallon collected the data. Jamadar, Ward, Parkes, and Sasan analyzed the data. Jamadar, Ward, Carey, and McIntyre wrote the first draft of the manuscript. All authors have reviewed and approved the final version.

#### **DISCLOSURES:**

The authors declare no conflict of interest. The funding source was not involved in the study design, collection, analysis, and interpretation of data.

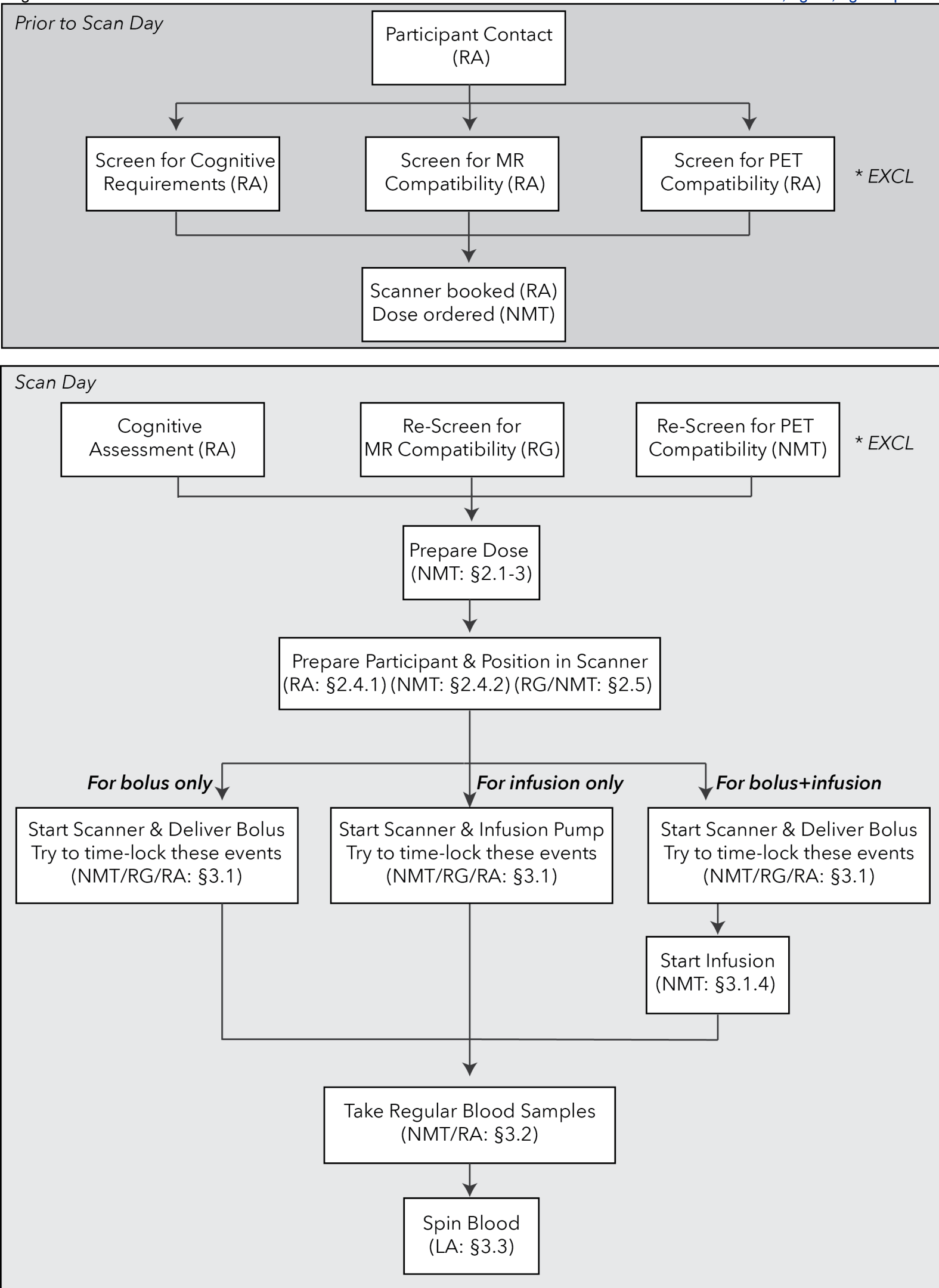
#### **REFERENCES:**

1. Heurling, K. et al. Quantitative positron emission tomography in brain research. *Brain Research*. **1670**, 220–234 (2017).
2. Chen, Z. et al. From simultaneous to synergistic MR-PET brain imaging: A review of hybrid MR-PET imaging methodologies. *Human Brain Mapping*. **39** (12), 5126–5144 (2018).
3. Jones, T., Rabiner, E. A. The development, past achievements, and future directions of brain PET. *Journal of Cerebral Blood Flow & Metabolism*. **32** (7), 1426–1454 (2012).
4. Kety, S. S. in *Metabolism of the nervous system*. 221–237 (Elsevier, 1957).
5. Sokoloff, L. The metabolism of the central nervous system in vivo. *Handbook of Physiology, section I, neurophysiology*. **3**, 1843–1864 (1960).
6. Harris, J. J., Jolivet, R., Attwell, D. Synaptic energy use and supply. *Neuron*. **75** (5), 762–777 (2012).
7. Mosconi, L. et al. FDG-PET changes in brain glucose metabolism from normal cognition to pathologically verified Alzheimer's disease. *European Journal of Nuclear Medicine and Molecular Imaging*. **36** (5), 811–822 (2009).
8. Pagano, G., Niccolini, F., Politis, M. Current status of PET imaging in Huntington's disease. *European Journal of Nuclear Medicine and Molecular Imaging*. **43** (6), 1171–1182 (2016).
9. Petit-Taboue, M., Landeau, B., Desson, J., Desgranges, B., Baron, J. Effects of healthy aging on the regional cerebral metabolic rate of glucose assessed with statistical parametric mapping. *Neuroimage*. **7** (3), 176–184 (1998).
10. Chugani, H. T., Phelps, M. E., Mazziotta, J. C. Positron emission tomography study of human brain functional development. *Annals of Neurology*. **22** (4), 487–497 (1987).
11. Phelps, M. E., Mazziotta, J. C. Positron emission tomography: human brain function and biochemistry. *Science*. **228** (4701), 799–809 (1985).
12. Zimmer, E. R. et al. [18 F] FDG PET signal is driven by astroglial glutamate transport. *Nature Neuroscience*. **20** (3), 393 (2017).
13. Roberts, R. P., Hach, S., Tippet, L. J., Addis, D. R. The Simpson's paradox and fMRI: Similarities and differences between functional connectivity measures derived from within-subject and across-subject correlations. *Neuroimage*. **135**, 1–15 (2016).
14. Horwitz, B. The elusive concept of brain connectivity. *Neuroimage*. **19** (2), 466–470 (2003).
15. Moses, W. W. Fundamental limits of spatial resolution in PET. *Nuclear Instruments and Methods in Physics Research Section A: Accelerators, Spectrometers, Detectors and Associated Equipment*. **648**, S236–S240 (2011).

16. Tomasi, D. G. et al. Dynamic brain glucose metabolism identifies anti-correlated cortical-cerebellar networks at rest. *Journal of Cerebral Blood Flow & Metabolism*. **37** (12), 3659–3670 (2017).
17. Hahn, A. et al. Quantification of task specific glucose metabolism with constant infusion of 18F-FDG. *Journal of Nuclear Medicine*. **57** (12), 1933–1940 (2016).
18. Hahn, A. et al. Task-relevant brain networks identified with simultaneous PET/MR imaging of metabolism and connectivity. *Brain Structure and Function*. **223** (3), 1369–1378 (2018).
19. Jamadar, S. D. et al. Simultaneous task-based BOLD-fMRI and [18-F] FDG functional PET for measurement of neuronal metabolism in the human visual cortex. *Neuroimage*. **189**, 258–266 (2019).
20. Rischka, L. et al. Reduced task durations in functional PET imaging with [18F] FDG approaching that of functional MRI. *Neuroimage*. **181**, 323–330 (2018).
21. Villien, M. et al. Dynamic functional imaging of brain glucose utilization using fPET-FDG. *Neuroimage*. **100**, 192–199 (2014).
22. Carson, R. E. PET physiological measurements using constant infusion. *Nuclear Medicine and Biology*. **27** (7), 657–660 (2000).
23. Carson, R. E. et al. Comparison of bolus and infusion methods for receptor quantitation: application to [18F] cyclofoxy and positron emission tomography. *Journal of Cerebral Blood Flow & Metabolism*. **13** (1), 24–42 (1993).
24. National Health and Medical Research Council. *National statement on ethical conduct in human research*. (2007).
25. Protection, A. R. ARPANSA-Code of practice for the exposure of humans to ionizing radiation for research purposes (2005).
26. Jenkinson, M., Beckmann, C. F., Behrens, T. E., Woolrich, M. W., Smith, S. M. Fsl. *Neuroimage*. **62** (2), 782–790 (2012).
27. Tustison, N. J. et al. N4ITK: improved N3 bias correction. *IEEE Transactions on Medical Imaging*. **29** (6), 1310 (2010).
28. Avants, B., Klein, A., Tustison, N., Woo, J., Gee, J. C. in *16th Annual Meeting for the Organization of Human Brain Mapping*.
29. Avants, B. B., Epstein, C. L., Grossman, M., Gee, J. C. Symmetric diffeomorphic image registration with cross-correlation: evaluating automated labeling of elderly and neurodegenerative brain. *Medical Image Analysis*. **12** (1), 26–41 (2008).
30. Klein, A. et al. Mindboggling morphometry of human brains. *PLoS Computational Biology*. **13** (2), e1005350 (2017).
31. Tustison, N. J. et al. Large-scale evaluation of ANTs and FreeSurfer cortical thickness measurements. *Neuroimage*. **99**, 166–179 (2014).
32. Avants, B. B. et al. A reproducible evaluation of ANTs similarity metric performance in brain image registration. *Neuroimage*. **54** (3), 2033–2044 (2011).
33. Burgos, N. et al. Attenuation correction synthesis for hybrid PET-MR scanners: application to brain studies. *IEEE Transactions on Medical Imaging*. **33** (12), 2332–2341 (2014).
34. Panin, V. Y., Kehren, F., Michel, C., Casey, M. Fully 3-D PET reconstruction with system matrix derived from point source measurements. *IEEE Transactions on Medical Imaging*. **25** (7), 907–921 (2006).

- 745 35. Jenkinson, M., Bannister, P., Brady, M., Smith, S. Improved optimization for the robust  
746 and accurate linear registration and motion correction of brain images. *Neuroimage*. **17**  
747 (2), 825–841 (2002).
- 748 36. Bludau, S. et al. Cytoarchitecture, probability maps and functions of the human frontal  
749 pole. *Neuroimage*. **93**, 260–275 (2014).
- 750 37. Amunts, K., Malikovic, A., Mohlberg, H., Schormann, T., Zilles, K. Brodmann's areas 17 and  
751 18 brought into stereotaxic space—where and how variable? *Neuroimage*. **11** (1), 66–84  
752 (2000).
- 753 38. Malikovic, A. et al. Cytoarchitectonic analysis of the human extrastriate cortex in the  
754 region of V5/MT+: a probabilistic, stereotaxic map of area hOc5. *Cerebral Cortex*. **17** (3),  
755 562–574 (2006).
- 756 39. Wilms, M. et al. Human V5/MT+: comparison of functional and cytoarchitectonic data.  
757 *Anatomy and Embryology*. **210** (5–6), 485–495 (2005).
- 758 40. Eickhoff, S. B., Heim, S., Zilles, K., Amunts, K. Testing anatomically specified hypotheses in  
759 functional imaging using cytoarchitectonic maps. *Neuroimage*. **32** (2), 570–582 (2006).
- 760 41. Eickhoff, S. B. et al. Assignment of functional activations to probabilistic cytoarchitectonic  
761 areas revisited. *Neuroimage*. **36** (3), 511–521 (2007).
- 762 42. Eickhoff, S. B. et al. A new SPM toolbox for combining probabilistic cytoarchitectonic maps  
763 and functional imaging data. *Neuroimage*. **25** (4), 1325–1335 (2005).
- 764 43. Everett, B. A. et al. Safety of radial arterial catheterization in PET research subjects. *Journal*  
765 *of Nuclear Medicine*. **50** (10), 1742–1742 (2009).
- 766 44. Takagi, S. et al. Quantitative PET cerebral glucose metabolism estimates using a single  
767 non-arterialized venous-blood sample. *Annals of Nuclear Medicine*. **18** (4), 297–302  
768 (2004).
- 769 45. Zanotti-Fregonara, P., Chen, K., Liow, J.-S., Fujita, M., Innis, R. B. Image-derived input  
770 function for brain PET studies: many challenges and few opportunities. *Journal of Cerebral*  
771 *Blood Flow & Metabolism*. **31** (10), 1986–1998 (2011).
- 772 46. O'Loughlin, S., Currie, G. M., Trifonovic, M., Kiat, H. Ambient temperature and cardiac  
773 accumulation of <sup>18</sup>F-FDG. *Journal of Nuclear Medicine Technology*. **42** (3), 188–193  
774 (2014).

Figure1

[Click here to access/download;Figure;Figure1.pdf](#)



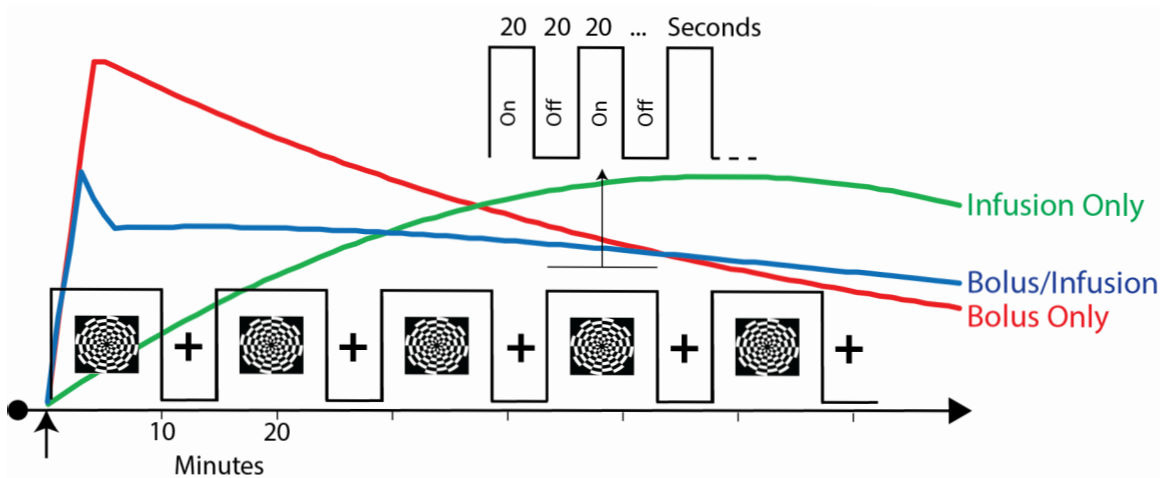
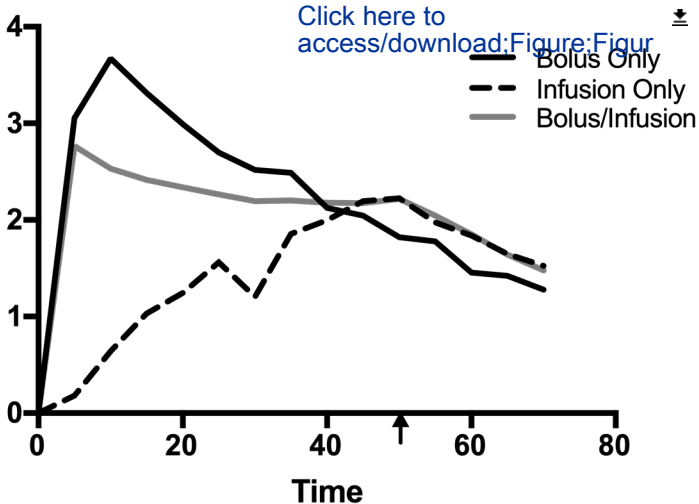
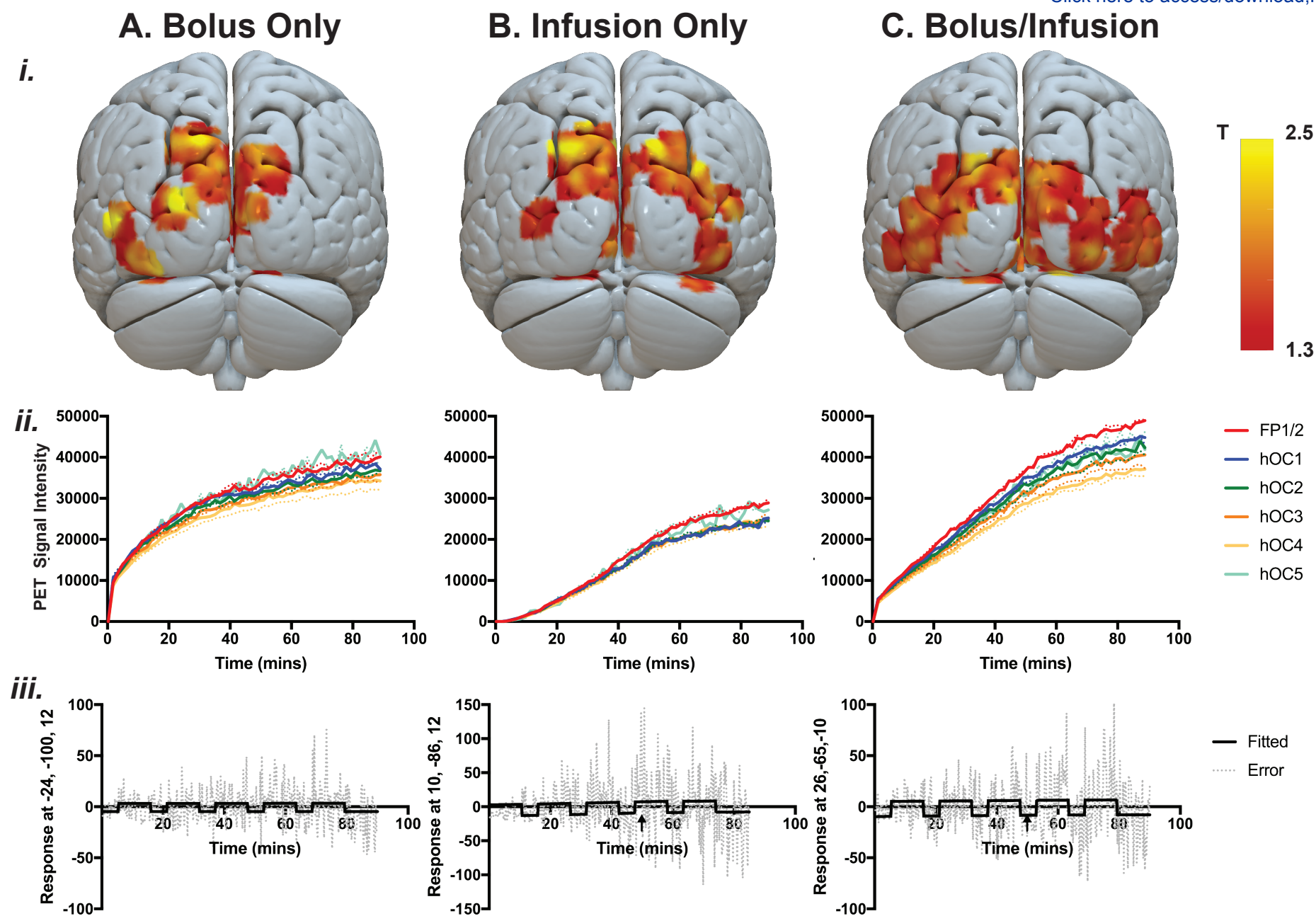


Figure3

Plasma Radioactivity  
Concentration kBq/cc

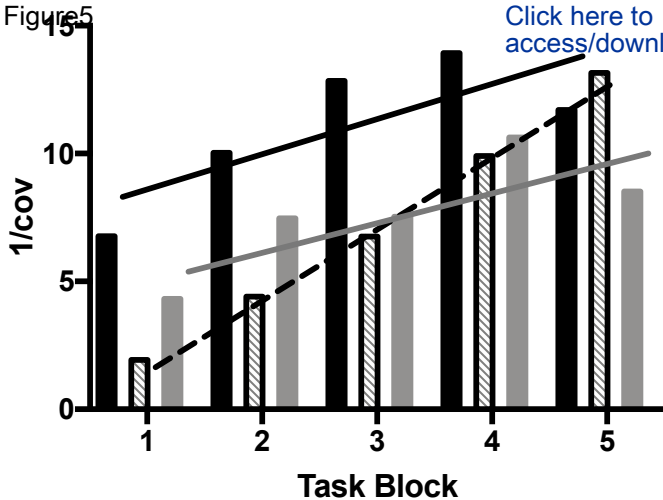









[Click here to access/download;Figure;Figure5.pdf](#)

Figure 5



-  Bolus Only
-  Infusion Only
-  Bolus/Infusion

	Participant 1	Participant 2	Participant 3
Administration protocol	bolus only	infusion only	bolus/infusion
Age (years)	18	19	19
Sex	F	M	F
Handedness	R	R	R
Years of Education	12	14	14
Current Axis I Psychiatric illness	None	None	None
History of Cardiovascular Disease	None	None	None
Regular Medication	None	None	None

## **Name of Material/Equipment**

### ***Blood Collection Equipment***

- 12-15 vacutainers
- 12-15 10mL LH blood collecting tubes

- 2-15 10mL Terumo syringe
- pre-drawn 0.9% saline flushes
- 12-15 5mL Terumo syringes

### ***Safety & Waste Equipment***

- Gloves
- waste bags
- cello underpads 'blueys' Underpads 5 Ply
- Blue Sharpie pen

### ***Dose Syringes***

- 5mL
- 20mL
- 50mL
- 1 Terumo 18-gauge needle
- 100mL 0.9% saline bag

### ***Radiochemistry Lab Supplies***

- Heraeus Megafuge 16 centrifuge; Rotor Bioshield 720
- Single well counter
- Pipette
- 12-15 plasma counting tubes
- 12-15 pipette tips
- 3 test tube racks
- 500mL volumetric flask and distilled water
- Synchronised clocks in scanner room, console and radiochemistry lab
- Haemoglobin Monitor
- Glucometre

### ***Cannulating Equipment***

- Regulation tourniquet
- 20, 22 and 24 gauge cannulas
- tegaderm dressings
- alcohol and chlorhexidine swabs
- 0.9% saline 10mL ampoules; for flushes
- 10mL syringes
- 3-way tap
- IV bung
- Optional extension tube, microbore extension set

### ***Scanner Room Equipment***

- Siemens Biograph 3T mMR
- Portable lead barrier shield
- Infusion pump BodyGuard 323 MR-conditional infusion pump
- Infusion pump tubing
- Lead bricks

### ***Other Equipment***

- Syringe shields
- Geiger counter Model 26-1 Integrated Frisker

Company	Catalog Number
Becton Dickinson, NJ USA	364880
Becton Dickinson	367526
Terumo Tokyo, Japan	SS+10L
Pfizer, NY, USA	61039117
Terumo Tokyo, Japan	SS+05S
Westlab, VIC, Australia	663-219
Austar Packaging, VIC, Australia	YIW6090
Halyard Health, NSW, Australia	2765A
Sharpie, TN, USA	S30063
Terumo Tokyo, Japan	SS+05S
Terumo Tokyo, Japan	SS+20L
Terumo Tokyo, Japan	SS*50LE
Terumo Tokyo, Japan	NN+1838R
Baxter Pharmaceutical, IL, USA	AHB1307
ThermoScientific MA, USA	75004230
Laboratory Technologies, Inc. IL, USA	630-365-1000
ISG Xacto, Vienna, Austria	LI10434
Techno PLAS; SA Australia	P10316SU
Expell Capp, Denmark	5130140-1
Generic	
Generic	
Generic	
EKF Diagnostic Cardiff, UK Haemo Control.	3000-0810-6801
Roche Accu-Chek	6870252001



CBC Classic Kimetec GmbH	K5020
Braun, Melsungen Germany	251644-03; 4251628-03; 4251601-03
3M, MN USA	1624W
Reynard Health Supplies, NSW Australia	RHS408
Pfizer, NY, USA	61039117
Terumo Tokyo, Japan	SS+10L
Becton Dickinson Connecta	394600
Safsite Braun PA USA	415068
M Devices, Denmark	IV054000

Siemens, Erlangen, Germany	
Gammasonics	Custom-built

Caesarea Medical Electronics	300-040XP
Caesarea Medical Electronics	100-163X2YNKS
Custom built	

Biodex, NY USA	Custom-built
----------------	--------------

Ludlum Measurements, Inc. TX USA	48-4007
----------------------------------	---------

## Comments/Description

Remain in sterile packaging until required to put blood in tube

Marked with the sample number (e.g., S1, S2...) and subsequently marked with the sample time (e.g., time 0 + x min [ $T_0+x$ ])

These are drawn up on the day of the study and capped with the ampoule that contained the saline

Remain in sterile packaging until ready to withdraw a blood sample

All objects arranged on a plastic chair inside the scanner room on the same side as the arm from which the blood samples will be taken. Biohazard and non-biohazard waste bags to be used. Gloves and waste bags to be easily accessible when preparing the radioactivity in the dispensing area and when pipetting the plasma samples. Biohazard and non-biohazard waste bags to be used. All waste generated is checked with the Geiger counter to ensure that radioactive contaminated waste is stored until it is safe to be disposed of according to Australian Radiation Protection and Nuclear Safety Agency

Remain in sterile packaging until ready for use. All syringes used in this facility have an additional 20% volume capacity above the stated volume on the packaging. This is important for the 50mL syringe

Remain in sterile packaging until ready to inject [ $^{18}\text{F}$ ]FDG into the saline bag

Remain in sterile packaging until ready to inject [ $^{18}\text{F}$ ]FDG

Relative Centrifugal Force = 724 Our settings are 2000RPM for 5mins. Acceleration and deceleration Complete daily quality control (includes background count) and protocol set to 18F and 4mins. Cross calibration is performed between the well counter, dose calibrator and scanner on a bi-monthly basis. We use a 100-1000  $\mu\text{L}$  set to 1000 $\mu\text{L}$ . It is calibrated annually.

Marked in the same manner as the LH blood tubes

Checked with a Geiger counter to ensure there is no radiation contamination on them

Need approximately 500mL of distilled water to prepare the reference for gamma counting

Synchronisation checks are routinely completed in the facility on a weekly basis

Manufacturer recommended quality control performed before testing on participant's blood sample.

Accu-Chek Performa is used to measure participant blood sugar levels in mmol/L. Quality control is performed daily using high and low concentration solution control test.

Check expiry dates and train NMT to prepare aseptically for cannulation.

MR-conditional lead barrier shield. Positioned at the 2000 Gauss line with the castors locked to provide additional shielding of the radioactivity connected to the infusion pump.

MR-compatible. This model is cleared for use on 1.5 and 3T scanners at 2000 Gauss with castors  
Tubing is administration set with an anti-siphon valve and male luer lock (REF 100-163X2YNKS).  
Tested for ferromagnetic translational force

There is a 5mL tungsten syringe shield that is MR-safe, as well as a 50mL lead shield that has been tested for ferromagnetic attraction prior to use in the MR-PET scanner. It is used to transport the radioactive dose from the radiochemistry lab into the scanner to minimise radiation exposure to the  
This is calibrated annually and used to monitor potential contamination and waste. It is not taken into the MR-PET scanner.



1 Atwell Center #300  
Cambridge, MA 02142  
Tel: 617.945.9051  
www.jove.com

## ARTICLE AND VIDEO LICENSE AGREEMENT

4. **Retention of Rights in Article.** Notwithstanding the exclusive license granted to JoVE in **Section 3** above, the Author shall, with respect to the Article, retain the non-exclusive right to use all or part of the Article for the non-commercial purpose of giving lectures, presentations or teaching classes, and to post a copy of the Article on the institution's website or the Author's personal website, in each case provided that a link to the Article on the JoVE website is provided and notice of JoVE's copyright in the Article is included. All non-copyright intellectual property rights in and to the Article, such as patent rights, shall remain with the Author.

5. **Grant of Rights in Video – Standard Access.** This **Section 5** applies if the "Standard Access" box has been checked in **Item 1** above or if no box has been checked in **Item 1** above. In consideration of JoVE agreeing to produce, display or otherwise assist with the Video, the Author hereby acknowledges and agrees that, Subject to **Section 7** below, JoVE is and shall be the sole and exclusive owner of all rights of any nature, including, without limitation, all copyrights, in and to the Video. To the extent that, by law, the Author is deemed, now or at any time in the future, to have any rights of any nature in or to the Video, the Author hereby disclaims all such rights and transfers all such rights to JoVE.

6. **Grant of Rights in Video – Open Access.** This **Section 6** applies only if the "Open Access" box has been checked in **Item 1** above. In consideration of JoVE agreeing to produce, display or otherwise assist with the Video, the Author hereby grants to JoVE, subject to **Section 7** below, the exclusive, royalty-free, perpetual (for the full term of copyright in the Article, including any extensions thereto) license (a) to publish, reproduce, distribute, display and store the Video in all forms, formats and media whether now known or hereafter developed (including without limitation in print, digital and electronic form) throughout the world, (b) to translate the Video into other languages, create adaptations, summaries or extracts of the Video or other Derivative Works or Collective Works based on all or any portion of the Video and exercise all of the rights set forth in (a) above in such translations, adaptations, summaries, extracts, Derivative Works or Collective Works and (c) to license others to do any or all of the above. The foregoing rights may be exercised in all media and formats, whether now known or hereafter devised, and include the right to make such modifications as are technically necessary to exercise the rights in other media and formats. For any Video to which this **Section 6** is applicable, JoVE and the Author hereby grant to the public all such rights in the Video as provided in, but subject to all limitations and requirements set forth in, the CRC License.

7. **Government Employees.** If the Author is a United States government employee and the Article was prepared in the course of his or her duties as a United States government employee, as indicated in **Item 2** above, and any of the licenses or grants granted by the Author hereunder exceed the scope of the 17 U.S.C. 403, then the rights granted hereunder shall be limited to the maximum

rights permitted under such statute. In such case, all provisions contained herein that are not in conflict with such statute shall remain in full force and effect, and all provisions contained herein that do so conflict shall be deemed to be amended so as to provide to JoVE the maximum rights permissible within such statute.

8. **Protection of the Work.** The Author(s) authorize JoVE to take steps in the Author(s) name and on their behalf if JoVE believes some third party could be infringing or might infringe the copyright of either the Author's Article and/or Video.

9. **Likeness, Privacy, Personality.** The Author hereby grants JoVE the right to use the Author's name, voice, likeness, picture, photograph, image, biography and performance in any way, commercial or otherwise, in connection with the Materials and the sale, promotion and distribution thereof. The Author hereby waives any and all rights he or she may have, relating to his or her appearance in the Video or otherwise relating to the Materials, under all applicable privacy, likeness, personality or similar laws.

10. **Author Warranties.** The Author represents and warrants that the Article is original, that it has not been published, that the copyright interest is owned by the Author (or, if more than one author is listed at the beginning of this Agreement, by such authors collectively) and has not been assigned, licensed, or otherwise transferred to any other party. The Author represents and warrants that the author(s) listed at the top of this Agreement are the only authors of the Materials. If more than one author is listed at the top of this Agreement and if any such author has not entered into a separate Article and Video License Agreement with JoVE relating to the Materials, the Author represents and warrants that the Author has been authorized by each of the other such authors to execute this Agreement on his or her behalf and to bind him or her with respect to the terms of this Agreement as if each of them had been a party hereto as an Author. The Author warrants that the use, reproduction, distribution, public or private performance or display, and/or modification of all or any portion of the Materials does not and will not violate, infringe and/or misappropriate the patent, trademark, intellectual property or other rights of any third party. The Author represents and warrants that it has and will continue to comply with all government, institutional and other regulations, including, without limitation all institutional, laboratory, hospital, ethical, human and animal treatment, privacy, and all other rules, regulations, laws, procedures or guidelines, applicable to the Materials, and that all research involving human and animal subjects has been approved by the Author's relevant institutional review board.

11. **JoVE Discretion.** If the Author requests the assistance of JoVE in producing the Video in the Author's facility, the Author shall ensure that the presence of JoVE employees, agents or independent contractors is in accordance with the relevant regulations of the Author's institution. If more than one author is listed at the beginning of this Agreement, JoVE may, in its sole



1 Alewife Center #200  
Cambridge, MA 02142  
Tel: 617.945.9051  
www.jove.com

## ARTICLE AND VIDEO LICENSE AGREEMENT

discretion, elect not take any action with respect to the Article until such time as it has received complete, executed Article and Video License Agreements from each such author. JoVE reserves the right, in its absolute and sole discretion and without giving any reason therefore, to accept or decline any work submitted to JoVE. JoVE and its employees, agents and independent contractors shall have full, unfettered access to the facilities of the Author or of the Author's institution as necessary to make the Video, whether actually published or not. JoVE has sole discretion as to the method of making and publishing the Materials, including, without limitation, to all decisions regarding editing, lighting, filming, timing of publication, if any, length, quality, content and the like.

12. **Indemnification.** The Author agrees to indemnify JoVE and/or its successors and assigns from and against any and all claims, costs, and expenses, including attorney's fees, arising out of any breach of any warranty or other representations contained herein. The Author further agrees to indemnify and hold harmless JoVE from and against any and all claims, costs, and expenses, including attorney's fees, resulting from the breach by the Author of any representation or warranty contained herein or from allegations or instances of violation of intellectual property rights, damage to the Author's or the Author's institution's facilities, fraud, libel, defamation, research, equipment, experiments, property damage, personal injury, violations of institutional, laboratory, hospital, ethical, human and animal treatment, privacy or other rules, regulations, laws, procedures or guidelines, liabilities and other losses or damages related in any way to the submission of work to JoVE, making of videos by JoVE, or publication in JoVE or elsewhere by JoVE. The Author shall be responsible for, and shall hold JoVE harmless from, damages caused by lack of sterilization, lack of cleanliness or by contamination due to

the making of a video by JoVE its employees, agents or independent contractors. All sterilization, cleanliness or decontamination procedures shall be solely the responsibility of the Author and shall be undertaken at the Author's expense. All indemnifications provided herein shall include JoVE's attorney's fees and costs related to said losses or damages. Such indemnification and holding harmless shall include such losses or damages incurred by, or in connection with, acts or omissions of JoVE, its employees, agents or independent contractors.

13. **Fees.** To cover the cost incurred for publication, JoVE must receive payment before production and publication of the Materials. Payment is due in 21 days of invoice. Should the Materials not be published due to an editorial or production decision, these funds will be returned to the Author. Withdrawal by the Author of any submitted Materials after final peer review approval will result in a US\$1,200 fee to cover pre-production expenses incurred by JoVE. If payment is not received by the completion of filming, production and publication of the Materials will be suspended until payment is received.

14. **Transfer, Governing Law.** This Agreement may be assigned by JoVE and shall inure to the benefits of any of JoVE's successors and assignees. This Agreement shall be governed and construed by the internal laws of the Commonwealth of Massachusetts without giving effect to any conflict of law provision thereunder. This Agreement may be executed in counterparts, each of which shall be deemed an original, but all of which together shall be deemed to be one and the same agreement. A signed copy of this Agreement delivered by facsimile, e-mail or other means of electronic transmission shall be deemed to have the same legal effect as delivery of an original signed copy of this Agreement.

A signed copy of this document must be sent with all new submissions. Only one Agreement is required per submission.

### CORRESPONDING AUTHOR

Name:	Sharna Jamadar	
Department:	Turner Institute for Brain and Mental Health	
Institution:	Monash University	
Title:	Dr	
Signature:		Date: 14/05/2019

Please submit a **signed** and **dated** copy of this license by one of the following three methods:

1. Upload an electronic version on the JoVE submission site
2. Fax the document to +1.866.381.2236
3. Mail the document to JoVE / Attn: JoVE Editorial / 1 Alewife Center #200 / Cambridge, MA 02140





100 Brookline Avenue  
Cambridge, MA 02142  
Tel: 617.945.9001  
www.jove.com

## ARTICLE AND VIDEO LICENSE AGREEMENT

Title of Article: **Constant Infusion Radiotracer Administration for High Temporal Resolution Positron Emission Tomography (PET) of the Human Brain: Application to [<sup>18</sup>F]-Fluorodeoxyglucose PET (FDG-PET)**

Author(s): **Shama D Jamadar, Phillip GD Ward, Alexandra Carey, Richard McIntyre, Linden Parkes, Disha Sasan, John Fallon, Shengpeng Li, Zhaolin Chen, Gary F Egan**

Item 1: The Author elects to have the Materials be made available (as described at <http://www.jove.com/publish>) via:

☒ Standard Access

☐ Open Access

Item 2: Please select one of the following items:

☒ The Author is **NOT** a United States government employee.

☐ The Author is a United States government employee and the Materials were prepared in the course of his or her duties as a United States government employee.

☐ The Author is a United States government employee but the Materials were NOT prepared in the course of his or her duties as a United States government employee.

## ARTICLE AND VIDEO LICENSE AGREEMENT

1. **Defined Terms.** As used in this Article and Video License Agreement, the following terms shall have the following meanings: "Agreement" means this Article and Video License Agreement; "Article" means the article specified on the last page of this Agreement, including any associated materials such as texts, figures, tables, artwork, abstracts, or summaries contained therein; "Author" means the author who is a signatory to this Agreement; "Collective Work" means a work, such as a periodical issue, anthology or encyclopedia, in which the Materials in their entirety in unmodified form, along with a number of other contributions, constituting separate and independent works in themselves, are assembled into a collective whole; "CRC License" means the Creative Commons Attribution-Non Commercial-No Derivs 3.0 Unported Agreement, the terms and conditions of which can be found at: <http://creativecommons.org/licenses/by-nc-nd/3.0/legalcode>; "Derivative Work" means a work based upon the Materials or upon the Materials and other pre-existing works, such as a translation, musical arrangement, dramatization, fictionalization, motion picture version, sound recording, art reproduction, abridgment, condensation, or any other form in which the Materials may be recast, transformed, or adapted; "Institution" means the institution, listed on the last page of this Agreement, by which the Author was employed at the time of the creation of the Materials; "JoVE" means MyJoVE Corporation, a Massachusetts corporation and the publisher of The Journal of Visualized Experiments; "Materials" means the Article and / or the Video; "Parties" means the Author and JoVE; "Video" means any video(s) made by the Author, alone or in conjunction with any other parties, or by JoVE or its affiliates or agents, individually or in collaboration with the Author or any other parties, incorporating all or any portion

of the Article, and in which the Author may or may not appear.

2. **Background.** The Author, who is the author of the Article, in order to ensure the dissemination and protection of the Article, desires to have the JoVE publish the Article and create and transmit videos based on the Article. In furtherance of such goals, the Parties desire to memorialize in this Agreement the respective rights of each Party in and to the Article and the Video.

3. **Grant of Rights in Article.** In consideration of JoVE agreeing to publish the Article, the Author hereby grants to JoVE, subject to Sections 4 and 7 below, the exclusive, royalty-free, perpetual (for the full term of copyright in the Article, including any extensions thereto) license (a) to publish, reproduce, distribute, display and store the Article in all forms, formats and media whether now known or hereafter developed (including without limitation in print, digital and electronic form) throughout the world, (b) to translate the Article into other languages, create adaptations, summaries or extracts of the Article or other Derivative Works (including, without limitation, the Video) or Collective Works based on all or any portion of the Article and exercise all of the rights set forth in (a) above in such translations, adaptations, summaries, extracts, Derivative Works or Collective Works and (c) to license others to do any or all of the above. The foregoing rights may be exercised in all media and formats, whether now known or hereafter devised, and include the right to make such modifications as are technically necessary to exercise the rights in other media and formats. If the "Open Access" box has been checked in Item 1 above, JoVE and the Author hereby grant to the public all such rights in the Article as provided in, but subject to all limitations and requirements set forth in, the CRC License.

Dear Prof Steindel,

Thank you for inviting a revision of our protocol paper. In this Letter, we respond in detail to each of the Reviewer comments.

Note:

Please note that during the course of revision, we identified a problem with one of the regions-of-interest (ROIs): the registration of Brodmann area 19 (BA19) with the most posterior occipital cortex was inaccurate. On further inspection, we realised that the atlas used to generate the ROI in the Wake Forest toolbox is based on a single-subject, which had been transformed between Talairach and MNI space (Maldjian et al., 2002). Despite continued widespread use (cited 4239 times), this atlas has been shown to have inferior registration compared to probabilistic atlases (e.g., Rodionov et al., 2009). We therefore have re-run the results using the Amunts/Zilles probabilistic atlas included in the SPM Anatomy Toolbox (Eickhoff et al. 2005).

The Amunts/Zilles atlas in the Anatomy toolbox has different parcellations compared to the Wakeforest Brodmann atlas. In the original submission, we created ROIs by combining BAs 17,18,19 for the occipital cortex, and compared to BA46 (dorsolateral prefrontal cortex, DLPFC) as a control region. In the new ROIs, we combined all human occipital cortex regions (hOC1-5) for the occipital cortex. The Amunts/Zilles atlas does not include BA46 (DLPFC), so we used frontopolar cortex (FP1,2) instead. The figures and relevant sections of the manuscript have been updated accordingly. All changes have been tracked in the revised submission.

With regards,

Sharna Jamadar

On behalf of the co-authors.

**Editorial comments:**

Manuscript:

1. Please take this opportunity to thoroughly proofread the manuscript to ensure that there are no spelling or grammar issues.
2. Please ensure that the manuscript is formatted according to JoVE guidelines—letter (8.5" x 11") page size, 1-inch margins, 12 pt Calibri font throughout, all text aligned to the left margin, single spacing within paragraphs, and spaces between all paragraphs and protocol steps/sub-steps.
3. Please print and sign the attached Author License Agreement (ALA). Please then scan and upload the signed ALA with the manuscript files to your Editorial Manager account.
4. For in-text formatting, corresponding reference numbers should appear as numbered superscripts after the appropriate statement(s). Please number references by appearance in the manuscript.
5. Please do not include footnotes.
6. Please reduce the summary to 10-50 words.

**Each of these changes have been made.**

Protocol:

1. Please ensure that all text in the protocol section is written in the imperative tense as if telling someone how to do the technique (e.g., "Do this," "Ensure that," etc.). The actions should be described in the imperative tense in complete sentences wherever possible.
2. Please convert centrifuge speeds to centrifugal force (x g) instead of revolutions per minute (rpm).
3. For each protocol step, please ensure you answer the "how" question, i.e., how is the step performed? Alternatively, add references to published material specifying how to perform the protocol action. If revisions cause a step to have more than 2-3 actions and 4 sentences per step, please split into separate steps or substeps.

**Each of these changes have been made.**

Specific Protocol steps:

1. 4: Please convert this section into numbered protocol steps, move it to the Results, or make it a supplemental file.
2. 4.1: Please do not cite papers that have not been accepted yet.

**The study-specific methods have been moved to the Results, and the reference to the as-yet-unaccepted manuscript has been removed.**

References:

1. As noted above, please put references in a numbered list by the order they appear in the manuscript.
2. Please ensure that the references appear as the following: [Lastname, F.I., LastName, F.I., LastName, F.I. Article Title. Source. Volume (Issue), FirstPage – LastPage (YEAR).] For more than 6 authors, list only the first author then et al.

**We have updated the format of the references.**

Table of Materials:

1. Please ensure the Table of Materials has information on all materials and equipment used, especially those mentioned in the Protocol.

**This has been done.**

### **Reviewer 1**

1. The manuscript should be examined as a whole to avoid colloquial usages of words and statements (i.e. line 373 "...and the concentration quickly decreases." How quickly? To and from what does it decrease? There are data to support this and language should be reserved for the discussion or omitted entirely.

**We have carefully read through the manuscript for colloquialisms. The line referred to here was intended as a qualitative description of the trend shown in Figure 2 (i.e., the radioactivity concentration curve). Note that the Journal Instruction to Authors requires statements about "how to interpret the data".**



We therefore have read through this section to ensure that when qualitative descriptions are given, this is made clear to the reader.

*Visual inspection of Figure 3 shows that the peak occurs within the first 10-mins of the protocol, and the concentration decreases thereafter.*

Further changes in response to this comment have been made throughout this section (all changes tracked), including:

*Qualitatively, across all protocols...*

*Visual inspection of Figure 4 suggests that in the bolus protocol...*

2. FDG-PET does not measure glucose metabolism. FDG-PET measures glucose uptake. Similarly, fMRI-BOLD does not measure brain activation. fMRI-BOLD measures the increased magnetic susceptibility due to deoxygenated hemoglobin, part of a cascade which occurs in high amounts due to activity related to neurovascular coupling. These pedantic points are absolutely critical to be understood and conveyed by the authors when attempting to discuss both methods, especially borrowing paradigms. Language should be corrected throughout to account for these nuanced points.

We agree with the Reviewer that accuracy of phrasing is important and we have carefully revised the manuscript to reflect this. With regards to the 'metabolism' point, we have made a number of revisions throughout (see tracked changes), but made it clear in the first paragraph that the measure of uptake is interpreted as an index of metabolism:

*In neuroscience, one of the most used radiotracers is [18F]-fluorodeoxyglucose (FDG-PET), which measures glucose uptake, usually interpreted as an index of cerebral glucose metabolism.*

While we did not refer to BOLD-fMRI as measuring 'brain activation' in the previous submission, we agree with the Reviewer that the standards in the literature, which use 'fMRI activity' as a synonym for 'brain activation', means that it is probable that some readers may misunderstand this. We therefore now make this clear at the end of the first paragraph:

*BOLD-fMRI is an indirect index of neural activity, and measures changes in deoxygenated haemoglobin that occur following a cascade of neurovascular changes following neuronal activity.*

3. A table describing the three participants is necessary, as although effects like flashing checkboards are generally quite large and should exceed the variance of subject selection, it is still important to present.

This information is provided in the (new) Table 2:

**Table 2: Demographic information for the three participants.**

	<i>Participant 1</i>	<i>Participant 2</i>	<i>Participant 3</i>
<i>Administration protocol</i>	<i>bolus only</i>	<i>infusion only</i>	<i>bolus/infusion</i>
<i>Age (years)</i>	<i>18</i>	<i>19</i>	<i>19</i>
<i>Sex</i>	<i>F</i>	<i>M</i>	<i>F</i>
<i>Handedness</i>	<i>R</i>	<i>R</i>	<i>R</i>
<i>Years of Education</i>	<i>12</i>	<i>14</i>	<i>14</i>
<i>Current Axis I Psychiatric illness</i>	<i>None</i>	<i>None</i>	<i>None</i>
<i>History of Cardiovascular Disease</i>	<i>None</i>	<i>None</i>	<i>None</i>
<i>Regular Medication</i>	<i>None</i>	<i>None</i>	<i>None</i>

4. Minor Concerns:

a. Line 97: fMRI BOLD can get to submillimeter resolution on an appropriate temporal scale, however PET has natural limitations due to "positron range". The authors might want to mention this.

This is now discussed as follows:

*With these developments, researchers have focused on improving the temporal resolution of FDG-PET to approach the standards of BOLD-fMRI (between ~0.5-2.5sec; note, the spatial resolution of BOLD-fMRI can approach sub-millimeter resolution, but the spatial resolution of FDG-PET is fundamentally limited to around 0.54mm FWHM due to the positron range; Moses, 2011).*

b. Line 134: A sample diagram explaining flow over time of a PET experiment would be very helpful, perhaps with explanations of block design where applicable, when comparing this method to previous dynamic PET methods.

This diagram is given in the (new) Figure 2.

c. Line 344: Please provide details regarding the specific program parameters used. What atlases were used for brain extraction, what method of non-linear normalization (I presume SyN if using ANTs)...What MCFLIRT parameters etc...

The required details have been added.

*T1-weighted structural images were neck-cropped using FSL-robustfov (Jenkinson, Beckmann, Behrens, Woolrich, & Smith, 2012), bias corrected using N4 (Tustison et al., 2010) and brain extracted using ANTs (Avants, Klein, Tustison, Woo, & Gee, 2010; Avants, Epstein, Grossman, & Gee, 2008) with OASIS-20 templates (Klein 2017, Tustison 2014). T1-weighted images were non-linearly normalised to a 2mm MNI template using ANTs (Avants et al., 2011) with the default parameter set defined by antsRegistrationSyN.sh.*

d. Line 386: See point above about opining.

**This line has been revised.**

e. Line 391: How were ROIs generated?

The ROIs were originally generated using the Wake Forest Pickatlas (wfu-pickatlas). As noted above. We discovered that the posterior registration with MNI space was very poor for BA19. We therefore re-generated ROIs using a probabilistic atlas (Eickhoff et al., 2005). This section has therefore been amended accordingly, as follows:

*An explicit mask of hOC1-5 (left & right hOC1,2,3d,3v,4d,4la4lp,4v,5; Amunts et al., 2000; Malikovic et al., 2007; Wilms et al., 2005; SPM Anatomy Toolbox v 2.2b Eickhoff et al., 2005; 2006; 2007) was included in the model to restrict the model estimation to regions of interest.*

f. Line 444: A CONSORT-like flow diagram of the 60 subjects would be useful. Patients with pacemakers can't get an MRI, patients with many issues cannot get FDG

CONSORT flow diagrams were developed for randomised control trials. The data collected here was not part of a randomised control trial, so it is beyond the scope to present the full details of all participants here. However, we have substantially extended Figure 1 to include CONSORT-like items illustrating the flow of procedures from first contact with participants. Note that we have also added further information about MR and PET screening in response to Reviewer 3 Comment 9.

*The NMT reviews safety for PET scanning (e.g., exclusion for pregnancy, diabetes, chemotherapy or radiotherapy in previous 8 weeks). The radiographer reviews participant safety for MRI scanning (e.g., exclusion for pregnancy, metallic implants (medical or non-medical), non-removable dental implants, claustrophobia).*

## **Reviewer 2**

1. The major problem is that the results obtained from the procedure do not support the interpretation and as such its efficacy is questionable. Moreover, the comparison is based just on a single subject for each method (3 in total), which does not permit this in an adequate manner. In the end, the reader is left with 3 different approaches, without knowing which of these should be used. However, the only way to speculate about the difference between the approaches can be achieved by increasing the number of subjects for each method.

The goal of the current manuscript is not to present a quantitative comparison of the three methods presented here. Rather – in accordance with the scope of JoVE – the goal here is to present the ‘specific and intricate details’ of the methods to acquire bolus, infusion, or hybrid bolus/infusion FDG-PET data. Thus, the results are ‘representative’, and demonstrate a ‘range of outcomes possible’ from variations in the protocol (see Instructions to Authors/manuscript template).

As outlined in the Introduction, we were invited to submit this paper given the technical complexity of the approach, and the increased interest in this method in recent times (see recent publications by Villien et al., 2014; Hahn et al., 2016; 2018; Rischka et al., 2018; Jamadar et al., 2019). This approach is consistent with the aims and scope of the Journal, which states that ‘JoVE is a methods-based journal. Thus [the Discussion] should be focused on the protocol and not the representative results’ (Instructions to Authors/manuscript template). We believe that the focus on detailed demonstration of this protocol is consistent with the aims of the Journal, and will be useful to new groups and students attempting to use this technique.

2. There are several major issues regarding the results (fig 3). The authors claim that the peak activity was found in the primary visual cortex (BA 17). This is not evident from fig 3i (primary visual is at the midline) and the coordinates given in fig 3iii are actually outside the gray matter for A and C and almost outside for B. As a consequence, the time course in fig 3iii and fig 4 need to be reworked to proper coordinates.

**This section has been revised substantially on the basis of the updated results (see note at start of the Rejoinder).**

The time course in fig 3iii is very difficult to interpret, I cannot see any clear model fits. What is actually shown? Is this the PET signal of the task?

**This is the fitted response and error of the GLM, so is not in a strict sense the time-course. We inaccurately referred to it as a time-course, so have changed this in the text (changes tracked throughout).**

e.g.,

***Figure 4iii shows the general linear model fitted response and error at the peak voxel for each subject...***

and

***...and so the fitted response is shown from the start of the first checkerboard period***

Please provide eg axial sections (instead of a 3D projection) and a clear presentation of the signal time course to support the above statements.

**Results presented in sections are now given in the Supplement (see also Reviewer 2 Comment 8).**

3. The results section is not easy to read, eg is there task and total uptake mixed in the first paragraph? Please refrain from comparison between hemispheres with such a low sample size. The term image-derived uptake is not used in the field, please rephrase.

**This section has been updated according to the revised results (see opening note). We have removed the reference to hemispheric comparisons. Note also that we have amended the Results section in response to Reviewer 1 (Comment 1; 4d) to make it clear when we are making a visual or qualitative description of results presented in the Figures.**

**We have replaced the term ‘image-derived uptake’ with ‘PET signal’, which we agree is more accurate (changes tracked throughout).**

4. In the results, what does the statement "model could not be estimated for the first rest period" mean? The model is estimated across the entire time course.

**Because the signal was close to zero at the beginning of the scan period for the infusion-only protocol, model estimation failed when taking into account the entire scan period. This was as expected as very little of the radiotracer has been injected during very early time-points for this protocol, and hence the signal/image intensity was not different from zero. We now clarify this in the manuscript, as follows:**

***Furthermore, for the infusion-only protocol, the signal during the first rest block was close to zero, as very little of the tracer had been administered during that time; and the general linear model estimation failed when taking into account this block. Thus, the general linear model was estimated for this participant starting with the first task block, and so the fitted response is shown from the start of the first checkerboard period.***

5. With the bolus only setting, do the authors imply that a bolus is almost equally feasible to detect dynamic task changes? This is somewhat counterintuitive as PET pioneers have shown signal changes when the task is done in the very beginning. Please explain.

**As mentioned in response to Reviewer 2 Comment 1, our goal was to present the protocol for the three methods. Like the Reviewer, we feel that a conclusion as to ‘which is best’ requires stronger data and more quantitative comparison than the three representative participants presented here. These are three methods that are either widely used (in the case of bolus) or are becoming more common (infusion and bolus/infusion), and so our goal is to present the acquisition protocol specifics for others to use.**

**The fact that we were able to estimate a dynamic task-based response across the scan period for the bolus protocol shows that it is at least possible to do so. However, examination of Figure 5 suggests that the best timeframe to do so is right in the beginning of the protocol, consistent with the work the Reviewer referred to. Also, Figure 5 suggests that the bolus/infusion approach may provide a relatively more stable SNR, as evident by the reduced slope of the line.**

**Therefore, to address this comment, and to reduce the risk that readers will misinterpret our point, we have added the following line to the Results:**

***Further studies are required to determine if these effects are sustained in a larger sample.***

6. Regarding the analysis, it is not clear why the PET signal of the occipital cortex was used as a covariate. This signal will most likely include task-specific activation from the checkerboard stimulus. However, this will cancel out a substantial amount of the variance, which should be explained by the model. This will largely reduce the task effects.

Averaged radiotracer uptake was included as a covariate to account for the overall change in signal due to the continued infusion of the radiotracer during the scanning period. This would result in overall increased signal unrelated to the task. We note that the community has not yet determined the best way to account for this effect. However, in response to this comment, we used the uptake in the FP1-2 control region as the covariate in the updated results.

7. SPM has numerous assumptions implemented which are not seen or controllable by the user. Eg the convolution with the HRF and an autoregressive model. One assumption for the latter is actually the application of a high pass, but this was deactivated by the authors.

All fMRI-specific options were deactivated in the analysis. This includes HRF convolution and autoregressive model, which is indeed possible to deactivate in SPM12 at the first-level. We have amended this sentence to explicitly include the HRF and autoregressive model:

*The model did not include global normalisation, high-pass filter, convolution with the haemodynamic response, autoregressive model or masking threshold*

8. The statistical threshold of  $T=0.1$  uncorrected (I assume this should be  $p=0.1$ ),  $k=50$  voxels, is not acceptable. Even at single subject level, a FWE correction should be applied, as this is done in fMRI with sufficient task effects.

We acknowledge that the threshold we present is liberal, however, we chose this threshold for several reasons.

First, as this is a demonstration of the protocol and the representative results, we wanted to show the range of values obtained at the individual level with the three protocols. Many of these values are sub-threshold at the individual level, but may reach significance in a group-level analysis. This is compatible with the Journal's Instructions to Authors, which states that representative results should "...demonstrate the range of outcomes possible".

Secondly, we disagree with the Reviewer that FWE with fMRI at the single subject level is routinely presented in the literature. In a short literature review, we found a range of liberal uncorrected thresholds for single-subject fMRI (e.g., Bertoldi et al. Neuroimage 2015 [ $p<.05$ ,  $p<.01$ ]; Smith et al. Neuroimage 2006 [ $Z=2$ , i.e.,  $p<.02$ ]) these thresholds would be considered liberal by comparison to group-level fMRI data. Others report unthresholded single-subject fMRI results (e.g., Zhang et al., 2006; Human Brain Mapping). So, while our single-subject fPET threshold could be considered liberal, analyses using similarly liberal thresholds have been reported in the literature for single-subject fMRI.

Thirdly, fPET is still in its infancy, with many parameters and standards still to be established, a formal examination and comparison of fPET SNR at different temporal resolutions has not been reported. Nor have comparisons been made with fMRI SNR. In such an environment, the presentation and exploration of single-subject level results with liberal thresholds is justified and even preferred. We do know that fPET SNR is low, and this varies across the scan period (see e.g., Figure 5 here). We therefore feel that the most transparent way

of presenting the current representative results is to use a liberal threshold showing the range of values obtained in the regions of interest.

Taking into consideration these points, and to ensure full transparency of the methods and results, we now present each individual's results at six additional thresholds in the Supplement. These results are shown in sections, as requested in Reviewer 2's Comment 2.

9. Based on the provided results, the interpretation of 16s temporal resolution is not supported at all. Thus, statements in the discussion like "we have demonstrated a superior temporal resolution of 16s..." and the title must be changed. Such statements are only feasible when directly assessing the effect of different resolutions.

We have carefully reviewed the manuscript and removed instances where our language may have inadvertently conveyed a value statement, such as the 'superior' resolution noted by the Reviewer.

e.g.,

*We have demonstrated a temporal resolution of 16-sec, time-locked to a stimulus*

And

*This temporal resolution compares favourably to current standards in the literature...*

We note that the manuscript title is: 'Radiotracer Administration for High Temporal Resolution Positron Emission Tomography (PET) of the Human Brain: Application to FDG-PET'. We do not think that the title inaccurately suggests a quantitative comparison in the results. However, we note that the infusion approach described here is often referred to as 'fPET' in the community, so we have changed 'PET' to 'fPET':

*Radiotracer Administration for High Temporal Resolution Positron Emission Tomography (PET) of the Human Brain: Application to FDG-fPET*

It is actually amusing to see how the authors managed to circumvent the work of Rischka et al., Neurolmage (2018). Still, this should be more accurately included for fairness, eg they used a task-locked setting (introduction) and achieved 12s (only a marginal note in the discussion).

It was not our intention to undersell or minimise the work of Rischka et al. Within the scope of the manuscript goals (see responses to Reviewer 2 Comments 1 & 5), we wished to highlight that this method is receiving increased attention through the work of the MGH (Villien et al. 2014), Viennese (Hahn et al., 2016; 2017; Rischka et al., 2018), and Australian (Jamadar et al., 2019) groups. Detailed comparisons of the findings between each study are beyond the scope of the manuscript. However, we note that of the existing studies, we actually discuss the Rischka paper the most extensively. For example, a sentence in the Introduction describes the work by Rischka et al as follows:

*Rischka et al. (2018) recently applied this technique using a 20% bolus plus 80% infusion. As expected the arterial input function quickly rose above baseline levels and was sustained at a higher rate for a longer*

*period of time, compared to results using an infusion only procedure (e.g., Jamadar et al., 2019; Villien et al., 2014).*

We also extensively discussed the Rischka paper in the Discussion. The previous phrasing in the Discussion (where we included the Rischka results in parentheses) may have incorrectly given the impression that we were not appropriately acknowledging the Rischka paper. We have therefore amended this section to read:

*This temporal resolution compares favourably to current standards in the literature: Hahn et al., 2016; 2018; Jamadar et al., 2019; Villien et al., 2014 report FDG-fPET with 1-min resolution; Rischka et al., 2018 achieved stable FDG-fPET results with a frame duration of 12sec using 20/80% bolus/infusion.*

10. Please confirm that the SPM effect of interest was a single time course (not one for checkerboard, one for rest) with 640s vs 320s (not 20s). How were the 320s rest actually defined, fixation or eyes closed as in their previous study?

This information has been added:

*This slow alternation provides FDG-fPET contrast; these timing parameters were entered into the first-level general linear models during the analysis. ... In this protocol, rest periods were eyes open, fixated on a cross centrally presented on the screen.*

11. A limitation section is clearly missing, eg mentioning sample size, lack of arterial sampling, missing quantification, etc.

A limitations section is now included in the Discussion.

*fPET as a method is relatively new (first published by Villien et al., 2014); and the data is relatively complex to acquire, compared to traditional neuroimaging approaches like static PET and MRI/fMRI. Thus, there is substantial scope for improvement of data acquisition protocols. Here, we have presented the acquisition protocol for 3 tracer administration protocols (bolus, infusion, bolus/infusion) and the representative results from individual subjects from each method. In our group, we do not perform arterial sampling, due to the invasiveness of the procedure, and also the requirement for an MD-qualified researcher on site. Our image analyses therefore do not benefit from the quantitative information provided by arterial sampling. Note that Hahn et al. (2016) found 'excellent' agreement between arterial and venous sampling for determining CMRGlc for constant-infusion FDG-fPET (also see Takagi et al., 2004; Everett et al., 2009; and Zanotti-Freonara et al., 2011; for discussion of arterial, venous, and image-derived input functions for PET). Other improvements of the protocol include reducing the requirement for staff to enter the scanner room while scanning is underway. This may affect the MR field and data quality, may increase the radiation exposure to staff, and also increase participant movement and disengagement from cognitive tasks. We are currently developing equipment for automatic blood sampling and measurement. Lastly, to*



***date, traditional PET modelling methods developed for static imaging (e.g., kinetic, Patlak), have not yet been adapted to take into account infusion-based administration. More work is required to update those mathematical models for application to fPET data.***

12. Regarding the description of the procedure, it is not at all advisable to take lead bricks into the MRI scanner room as these bricks may also contain steel.

**The lead bricks that were purchased for the facility were tested for ferromagnetic attraction prior to use in the MR-PET scanner. The bricks showed no magnetic translation upon testing. The bricks are not moved during the scan period, so will not have a variable effect on the magnetic field within-scan. Also, there is no possibility of the bricks being moved due to magnetic translation, as the weight of the lead far exceeds any trace amounts of ferrous material in the bricks.**

Please comment on the MR-compatibility of the pump.

**This has been added to the Table of Materials:**

***This model is cleared for use on 1.5 and 3T scanners at 2000 Gauss with castors locked.***

Furthermore, there are several instances where radiation burden to the staff can and should be reduced: Measure the activity in a smaller syringe in an activity meter, put the fluid in a 50ml syringe and fill it to the volume needed with saline; refrain from priming the tube and rather fill it with saline. Therefore, handling with the bag, priming activity and the calibration mixture is unnecessary; administer the bolus from the pump.

**We developed our protocol of dose preparation according to the ALARA (as low as reasonably achievable) principle. We argue that our method reduces the risk of user error, spillage and needle-stick injury; by comparison to the method proposed by the Reviewer. We find that having the correct concentration in the saline bag enables us to fill a 50mL syringe in a more timely and safe manner than adding activity to a 50mL syringe, and then subsequently diluting it. This method would involve mixing 50mL syringe to evenly disperse the activity, increasing exposure to the technologist.**

13. It should be mentioned that subjects have to fast for at least 4 hours prior to the scan and are only allowed to drink water and unsweetened beverages.

**This is now mentioned in the participant preparation section:**

***Participants are advised to fast for 6 hours, and to consume only water (around 2 glasses), prior to the scan.***

14. How could the authors put 60mL of the FDG/saline solution in a 50mL syringe (2.1.4.2)?

**Somewhat counterintuitively, 50mL Terumo syringes are marked to a 60mL volume. Terumo add 20% capacity above the listed capacity on all models of**

their syringes. We could not source hand-injectable syringes larger than the “50mL” syringe. We now note this in the protocol.

*(Note that it is possible to draw a 60mL volume in a 50mL syringe, as Terumo syringes are marked to 20% above the labelled volume; i.e., 50mL syringe is marked to 60mL volume).*

How could the 60mL syringe be placed in the pump?

There is a giving set that is threaded in the pump. It has a connector that can be screwed into the Luer Lock tip of the syringe. There is a plastic holder that attaches to the IV pole that the syringe can sit on securely above the pump. The other end of the giving set is connected to the participant’s cannula.

Why can the 50mL syringe not be calibrated?

The 50mL syringe is very large and therefore does not easily fit into the dose calibrator. We find that it is more accurate to do a pre- and post-calibration of the radioactivity in a 5mL syringe first and then add it to the 100mL saline bag. That means that we have a known activity in a known concentration at a specific time. We have amended the protocol to make this clear.

*This syringe is not calibrated, as the concentration of the radioactivity is known from the time it was added to the saline bag (step 2.1.3)*

15. The NMT should not open the door of the scanner room, move around in the scanner room, go close to the gantry or withdraw blood directly from the arm during an active MR measurement, so that the magnetic field is not altered.

We note that the scanner room has two doors, in the form of an RF interlock, to eliminate interference to the MR images when opening the doors during MRI scanning. We also now mention this in the manuscript as a potential future improvement:

*Other improvements of the protocol include reducing the requirement for staff to enter the scanner room while scanning is underway. This affects the MR field and data quality, may increase the radiation exposure to staff, and also increase participant movement and disengagement from cognitive tasks.*

16. The description of the blood samples could be improved. Eg it should be mentioned that with a bolus an automatic blood sampling system is advisable to capture the initial activity peak.

This is now mentioned in the limitations/future improvements section:

*Manual blood sampling, whether arterial or venous, requires staff to enter the scanner room while scanning is underway. Most scanners have an RF interlock for the scanner room, which enables staff to access the room during scanning without causing electromagnetic interference artefacts in the MR images. However, staff entering the room during the scan may increase the radiation exposure to staff, may cause participant discomfort, and also increase participant movement and disengagement from cognitive tasks. These factors encourage the collection of as few samples as necessary. We have*

***found that samples taken every 5-10 minutes, whilst the dose is administered, is sufficient to observe the low-frequency blood dynamics expected from the three protocols examined here. However, this sampling rate limits the ability to quantify high-frequency temporal characteristics, particularly the exact size and shape of the peak following bolus administration. Where such characteristics are of importance the use of automated blood sampling equipment may be beneficial.***

What is meant by "regular" in 3.2?

**We mean “recurring at uniform intervals of time”. This has been changed to:**

***Take blood samples at regular intervals***

The whole blood analysis is not described in the manuscript although it is important for absolute quantification.

**This analysis was not conducted, and we have not presented quantitative image analyses in the manuscript.**

The authors jump from bringing blood samples to the lab to spinning (centrifuging?) the blood.

**We are not sure which section this comment refers to. The section about blood spinning has been placed in its own section, separate from the previous, as it is the responsibility of a different technician. i.e., we move from section 3.2.7 (NMT), where the sample is taken into the lab; to 3.3 (LA), where the procedure for spinning is described. We think this is a logical flow for the procedure.**

Furthermore, it is not clear what pre- and post-samples are and why the blood has to be analyzed in general.

**‘Pre- and post-sample’ was a typo and has been removed. The blood is measured to quantify plasma serum radioactivity. This is now explicitly stated:**

***We sample blood to quantify plasma serum radioactivity for subsequent quantification of PET images.***

What do the authors mean by "centrifuge at any time"?

**This is now clarified:**

***The blood sample can be placed in the centrifuge as the availability of staffing resources permits, since we note the time that the blood sample was taken, and the time it was counted***

It is important that whole blood is measured prior to centrifuging the blood sample.

**We do not measure whole blood because we are only interested in plasma serum levels.**

It should be mentioned that plasma is pipetted in step 3.3.4.

**This is noted:**

***Steadily pipette 1000µL plasma from the blood***

Although the authors write that the time should be recorded when the measurement in the well counter starts, it should also be mentioned why this is necessary (eg adjustment to PET start).

**This is noted:**

***This is required for subsequent correction to PET acquisition start time.***

Furthermore, a calibration between the PET/MR and the well counter has to be performed.

**This is now stated in the Table of Materials.**

***Cross calibration is performed between the well counter, dose calibrator and scanner on a bi-monthly basis.***

17. How was the amount of administered dose calculated?

**We are unsure which detail the Reviewer is specifically requesting. Details of dose calculation is given in the Protocol:**

***(Section 2.1.2) Calculate the dose that will be diluted into the administered solution (saline). In our protocol, we administer a total dose of 260MBq to the participant over 95mins... Using equation 1, solve for  $A_0$ ...***

**It is also possible that the Reviewer is referring to the selection of the 260MBq FDG. This was chosen in order to stay within the Category IIb risk assessment for radiation exposure according to ARPANSA guidelines. We now note this in the protocol:**

***This dose was chosen to limit radiation exposure to 4.9mSv, to keep within the 'low level risk' categorisation according to Australian Radiation Protection and Nuclear Safety Agency (ARPANSA) guidelines for exposure of humans to ionising radiation (2005).***

18. Subjects should only drink water prior to punctation if necessary since the urge to urinate will lead to head movement and in the worst case to scan abortion (as mentioned by the authors).

**We review the balance between finding veins and the need to urinate in the Discussion, as noted by the Reviewer.**

### **Reviewer 3**

1. The authors should provide additional details regarding data normalization, validation of venous blood sampling, and FDG modeling. The use of venous blood sampling should be discussed in further details.

**We fully address these points in the specific comments the Reviewer makes below, specifically, Comments 10, 13, 14, 15, 17. Note the following changes made in the manuscript:**

***Note that Hahn et al. (2016) found 'excellent' agreement between arterial and venous sampling for determining CMRGlc for constant-infusion FDG-fPET (also see Takagi et al., 2004; Everett et al., 2009; and Zanotti-Freonara et al., 2011; for discussion of arterial, venous, and image-derived input functions for PET).***

...

***Note that protocols that use arterial sampling will find a peak plasma concentration within the first minute; the delay here is because the first blood sample was taken at 5-mins post-bolus***

...

***Furthermore, for the infusion-only protocol, the signal during the first rest block was close to zero, as very little of the tracer had been administered during that time; as such model estimation failed when taking into account this block. Thus, the model was estimated for this participant starting with the first task block***

**The term ‘model’ has been clarified throughout as ‘general linear model’ (changes tracked).**

In addition, the article presents the results for 4 ROIs but in clinical environment, multiple regions are analyzed via brain atlas and spatial normalization techniques. This approach should be assessed since the 16-second temporal resolution may not provide sufficient signal for atlas-based analysis.

**Full assessment of temporal resolution is beyond the scope of the current manuscript (see also responses to Reviewer 2). Individual subject images were normalised to the individual’s T1 MRI and normalised into MNI space:**

***A mean FDG-PET image was derived from the entire dynamic timeseries and rigidly-normalised to the individual’s high-resolution T1-weighted image using ANTs (Avants et al., 2011). The dynamic FDG-fPET images were then normalised to MNI space...***

**We agree that in a clinical environment, different approaches are used. We now note this in the manuscript.**

***In the clinical environment, multiple regions are analysed using brain atlases***

2. Line 89: The author should reconsider the use of the word "metabolism". Routine clinical scans are static and are acquired after a long period of uptake and glucose metabolism is rarely determined in clinical environments. Glucose uptake via the Standard Uptake Value (SUV) is generally determined and should be considered instead of metabolism.

**We agree; Reviewer 1 (Comment 2) raised a similar point and we have made revisions (changes tracked) throughout the manuscript.**

**e.g.,**

***In neuroscience, one of the most used radiotracers is [18F]-fluorodeoxyglucose (FDG-PET), which measures glucose uptake, usually interpreted as an index of cerebral glucose metabolism.***

3. Line 101: In comparison to fMRI, static PET is similar to resting state or default mode network (DMN) determined from fMRI, and there is considerable interest in the DMN.

**We respectfully disagree. We do not believe that static PET scan is similar to resting state fMRI.**

**From a cognitive psychology viewpoint, we agree with the Reviewer: using traditional bolus acquisition methods (i.e., bolus -> uptake while quietly resting -> PET scan while quietly resting), the resulting PET image represents the integral of all cognitive activity occurring within the uptake and scanning periods. Thus, from this viewpoint, we agree that the *cognitive process of interest* is analogous to resting-state fMRI.**

**However, when considering how the data is analysed, there are subtle but important differences in the inferences that can be drawn from static PET versus fMRI. Resting-state fMRI is usually analysed by examining covariation of the time-courses between regions *within-subjects*. Group-level results are obtained by averaging or calculating similarities across subjects. Note we say 'usually analysed' as resting-state fMRI is sometimes calculated across-subjects, which the Roberts et al. paper shows does not yield the same results as within-subjects analyses. Using static PET, it is not possible to examine covariation between time-courses, because by definition, there is no temporal information in the static measure. Thus, resting-state fMRI takes into account within-subject variation across time, whereas resting-state static PET takes into account across-subject variation. This limitation of static PET is the motivation for development of the fPET technique presented here.**

**Also, if this topic is beyond the scope of this manuscript (footnote 1), then this topic should be removed completely.**

**The footnote has been removed.**

**4. Line 105-109: The conclusion about the inability to use bolus FDG-PET as a biomarker for disease is too bold of a statement and should be deleted or reduced in tone.**

**The statement has been rephrased:**

***While it is debatable what exactly across-subject connectivity actually measures (Horwitz, 2003), it is clear that measures calculated across-but not within-subjects cannot be used as a biomarker for disease states, or used to examine the source of individual variation.***

**5. Line 151: Is there a HRC approval # to include?**

***This protocol has been reviewed and approved by the Monash University Human Research Ethics Committee (approval number CF16/1108 – 2016000590), in accordance with...***

**6. Line 189: What is meant by "calibrate this 20 mL syringe"? Please be more specific.**

**The syringe is calibrated as a record of activity in a known volume. This a reference check to ensure the radioactivity has evenly dispersed within the 100mL saline bag. This is now explicitly stated:**

***The syringe is calibrated as a reference check to ensure the radioactivity has evenly dispersed within the saline bag.***

7. Line 191: Why can't this syringe be calibrated? Please provide a very brief explanation.

**This has been clarified in response to Reviewer 2 Comment 14.**

8. Line 227: The cannula section should specifically mention the use of two cannulas, one for injection and one for blood sampling.

**This is now noted:**

***Two cannulas are required: one for dose administration, the other for blood sampling.***

9. Line 251: Since this is PET/MRI, the document should briefly address MRI safety considerations (it does address hearing protection due to MRI, which is good).

**This was briefly mentioned in an earlier section, but has been elaborated to make the issue clear to the reader:**

***NMT and radiographer conduct safety screens: The NMT reviews safety for PET scanning (e.g., exclusion for pregnancy, diabetes, chemotherapy or radiotherapy in previous 8 weeks). The radiographer reviews participant safety for MRI scanning (e.g., exclusion for pregnancy, metallic implants (medical or non-medical), non-removable dental implants, claustrophobia).***

10. Line 278: Since this is venous blood sampling instead of arterial blood sampling, the validity of using venous blood should be presented. There is several factors that must be considered when using venous blood for determining plasma concentration and glucose metabolism. Also, please discuss the sampling time and # of samples.

**A full comparison of arterial versus venous blood sampling is beyond the scope of the current manuscript. We note however that Hahn et al. (2016) previously found that venous samples provide a good approximation for arterial data in FDG-fPET. This is now noted in the Discussion:**

***Note that Hahn et al. (2016) found 'excellent' agreement between arterial and venous sampling for determining CMRGlc for constant-infusion FDG-fPET (also see Takagi et al., 2004; Everett et al., 2009; and Zanotti-Freonara et al., 2011; for discussion of arterial, venous, and image-derived input functions for PET).***

**We have also expanded the discussion regarding the sampling time and number of samples in the Discussion:**

***Manual blood sampling, whether arterial or venous, requires staff to enter the scanner room while scanning is underway. This may affect the MR field and data quality, may increase the radiation exposure to staff, may cause participant discomfort, and also increase participant movement and disengagement from cognitive tasks. These factors***

***encourage the collection of as few samples as necessary. We have found that samples taken every 5-10 minutes whilst the dose is administered is sufficient to observe the blood dynamics expected from the three protocols examined here. However, this sampling rate limits the ability to quantify high-frequency temporal characteristics, particularly the exact size and shape of the peak following bolus administration. Where such characteristics are of importance the use of automated blood sampling equipment may be beneficial.***

11. Line 322: May want to consider just indicating that the full results will be reported in a future publication (drop the "Ward et al")

**This line has been removed in response to the Editor's Comment.**

12. Line 336: Indicate the scanner type, vendor and model.

**This information has been added:**

***MR and PET images were acquired on a Siemens (Erlangen, Germany) 3T Biograph mMR***

13. Line 372: Peak arterial plasma concentration is observed within the first minute, however you note that venous blood peaks at 5 minutes, which is the first blood sample. This difference should be noted since it might be confusing to those who generally use arterial blood sampling or arterialized venous blood.

**This has been added:**

***Note that protocols that use automated sampling at a rate of less than 1min will likely find a peak plasma concentration within the first minute; the delay here is because the first blood sample was taken at 5-mins post-bolus***

14. Line 413: Please include a brief description and details of the FDG model used to determine the glucose metabolism (e.g., Patlak, irreversible or reversible, 3 or 4 rate constants)

**Here, we do not model FDG metabolism. We believe our imprecise use of the term 'model' has led to misunderstanding. Here, we mean the general linear model estimated as described in the Study-Specific Methods. We have made the following amendments to address this:**

***Individual-level parameter maps from the general linear model***

**And**

***very little of the tracer had been administered during that time; as such general linear model estimation failed... Thus, the general linear model was estimated...***



We've updated the term 'model' throughout the manuscript to clarify that we mean 'general linear model' (changes tracked), and that we do not mean the modelling of glucose metabolism.

The Reviewer raises an important point with regard to application of traditional PET modelling techniques (e.g., kinetic and Patlak) to infusion-based data. We therefore mention this important point in our (new) limitations/future improvements section in the Discussion:

*Lastly, traditional PET modelling methods were developed for static imaging (e.g., kinetic, Patlak). More work is required to update those mathematical models for application to fPET data.*

15. Line 430: A "superior" temporal resolution of 16-sec is indicated but this is not strictly accurate since for the infusion-only protocol, the signal was too low for the first period for 16-sec temporal resolution

**This line has been removed in response to Reviewer 2 Comment 9. We also note that in response to Reviewer 2, we more fully discuss the low signal for the infusion-only protocol in the Results.**

*Furthermore, for the infusion-only protocol, the signal during the first rest block was close to zero, as very little of the tracer had been administered during that time; as such model estimation failed when taking into account this block. Thus, the model was estimated for this participant starting with the first task block*

16. Line 457: How does patient temperature (i.e., shivering) impact uptake for the various protocols? This is an important variable to control during scanning, in general.

**We agree, and now elaborate this point in the protocol:**

*The participant should be covered with a disposable blanket to maintain a comfortable body temperature.*

**And the Discussion:**

*Previous studies have shown that ambient temperature can influence artefactual activity in FDG-PET scans (O'Loughlin et al., 2014).*

17. Line 465: Please explain further since this sentence is confusing. Why would the image-derived uptake be consistent with plasma-based measures (venous blood measures)? What does this really mean?

**This line has been re-phrased in the updated results (see opening note to this Rejoinder).**

SCAN & SAMPLES

FDG Dose: \_\_\_\_\_

CLOCK TIMES:

Bolus Time: \_\_\_\_\_

Infusion Start: \_\_\_\_\_

Task Start: \_\_\_\_\_

Infusion End: \_\_\_\_\_

Blood Samples:

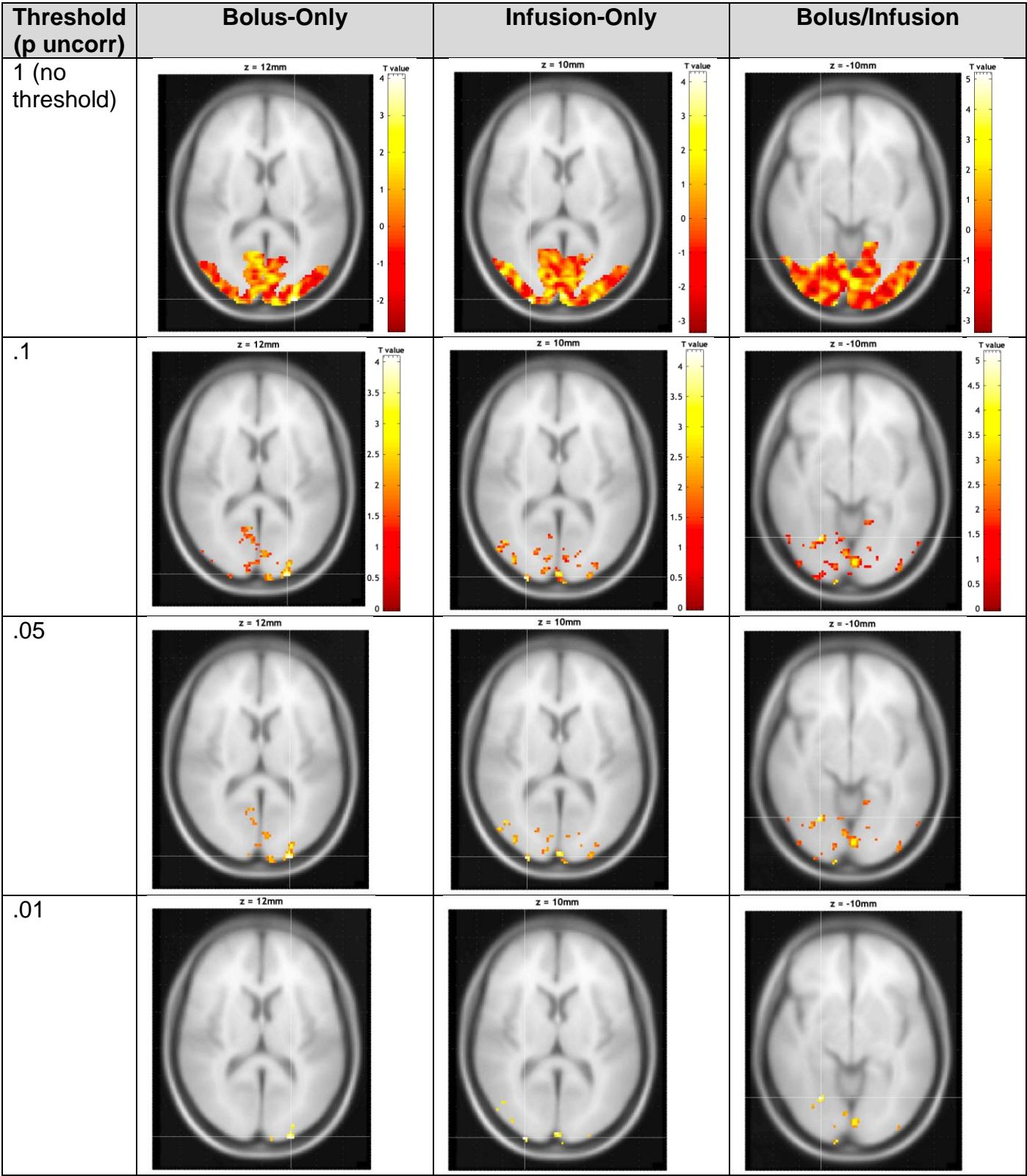
	Predicted <sup>a</sup> RESEARCHER	Actual <sup>b</sup> RESEARCHER	Measurement LAB TECH	Notes
TIME 0 <sup>c</sup>				
TIME 1				
TIME 2				
TIME 3				
TIME 4				
TIME 5				
TIME 6				
TIME 7				
TIME 8				
TIME 9				
TIME 10				

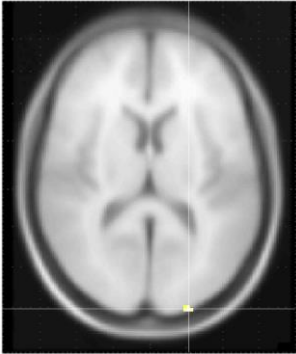
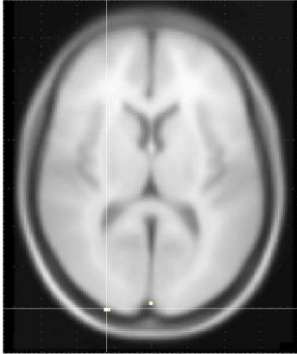
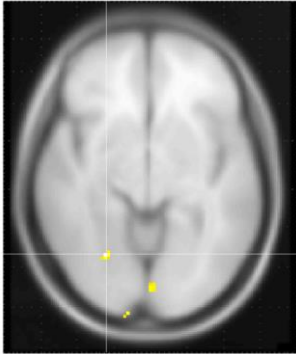
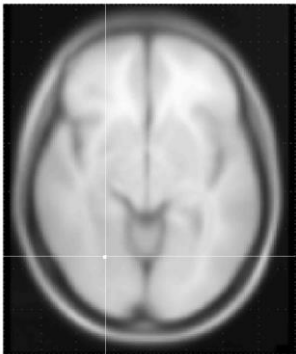
<sup>a</sup> Predicted time extrapolated from Time 0.  
<sup>b</sup> Actual time sample taken, indicated by “thumbs up” of person sampling blood  
<sup>c</sup> Time 0 = Infusion time + 5 mins

Supplement 2

Variability in statistical parameter maps with different statistical thresholds

Results for each individual at a range of thresholds (each k=0 voxels). The figure presented in the main manuscript shows  $p(\text{uncorr}) = 0.1$ . For each individual, the cross-hairs are centred at the peak voxel. For  $p < .05$ , .01, .001, and FWE  $p < .05$ , the colourbar is identical to that shown for  $p < .1$ .



.001	 <p>z = 12mm</p>	 <p>z = 10mm</p>	 <p>z = -10mm</p>
FWE corrected p<.05	no significant voxels	no significant voxels	 <p>z = -10mm</p>